

MARS EXPRESS ANALYZER OF SPACE PLASMAS AND ENERGETIC ATOMS (ASPERA-3) ELECTRON SPECTROMETER (ELS) CHARACTERIZATION

SwRI Project No. 15-03561

Contract No. NASW-00003

Prepared by



SOUTHWEST RESEARCH INSTITUTE®

Space Science and Engineering Division

6220 Culebra Road, San Antonio, Texas 78238-5166

TABLE OF CONTENTS

1.	Background.....	1
2.	Characterization at SwRI.....	1
2.1	Theoretical Modeling.....	2
2.2	ELS Characterization.....	5
2.2.1	ELS MCP Voltage Scans.....	6
2.2.2	Azimuth Scans.....	6
2.2.3	Elevation Scans.....	7
2.3	Ni-63 Tests.....	8
2.4	Characterization Summary.....	8
3.	MSSL Calibration of ELS.....	10
4.	ELS Calibration.....	10

LIST OF FIGURES

Figure 1.	Theoretical ELS Azimuthal Response.....	2
Figure 2.	Theoretical ELS Energy Response.....	3
Figure 3.	Theoretical ELS Elevation Response.....	4
Figure 4.	Simulated Response of Modeled ELS Measuring Expected Mars Ionospheric Electron Plasma.....	5
Figure 5.	ELS MCP Voltage Scan using Electron Gun.....	6
Figure 6.	ELS Azimuth Scan using Electron Gun.....	7
Figure 7.	ELS Sector Deflection Voltage Variation Showing Width of the Measured Voltage Response.....	8
Figure 8.	ELS Sector Resolution Determined from the Energy Response.....	9
Figure 9.	ELS Sector K-Factor Determined from the Energy Response.....	9

1. Background

The Electron Spectrometer (ELS) is the electron instrument for the Analyzer of Space Plasmas and Energetic Atoms (ASPERA-3) experiment flown on the Mars Express spacecraft. SwRI is responsible for the design and fabrication of the ELS instrument. The ELS calibration is performed by MSSL; however, SwRI characterized the ELS instrument to ensure that it performed correctly.

The ELS instrument was complete in its flight configuration for this characterization. The ELS housing was blackened and contained active MCPs in a chevron configuration. The ELS deflection system selectively determines particles that make a signal on the MCP sensor. The output from the MCPs activates anodes. The signals from each anode are amplified and shaped. The resulting output is sent to the data processing unit (DPU) for accumulation. The MCP signal is controlled by an MCP bias voltage, which is set by the DPU. The ESA deflection voltage and protection grid voltage, also supplied by the DPU, control the particle selection.

ELS characterization consists of four types of scans, three of them with an electron beam and one with a nuclear source. For tests with the electron beam, a narrow ESA deflection sweep is used to highlight the instrument response. The first test is a scan through the MCP bias voltages and is used to determine the MCP operating level for ELS. The second scan is through the azimuth. The azimuth test is meant to test the azimuthal response of ELS and relative intensities of the electron beam response on each anode. The third scan is in elevation and is meant to check both the elevation and voltage (energy) responses of ELS. The fourth test is performed with the nuclear source and checks both the inner anode stability and response to an absolute electron flux.

While under all test scans, all anode outputs are monitored to check for instrument crosstalk and to examine the instrument background. Instrument background is expected to be higher in these tests than in space because adequate outgassing is not achievable with these tests due to the shortness of their duration. However, background values are expected to decrease throughout these tests.

ELS output pulses are a positive +5V out, 250-nanosec wide square wave pulse. The output signals from each sector should be the same. Differences in signal quantity reflect slight differences in machining, alignment, and copper black coating of ELS and time differences in the stability of the electron beam. Differences in each sector should be revealed during a full calibration at MSSL and may not be evident from this characterization.

2. Characterization at SwRI

Prior to the characterization procedure, high voltage tests of the MCP and deflection system were conducted. The goal of the high voltage test is to prove that the MCP and the ELS instrument can withstand the high voltage required to operate the MCP. High voltage tests are also conducted to ensure that there will be no breakdown of high voltage within the instrument. These tests were performed at room temperature as well as at temperature extremes (hot and cold) required for ELS operation.

During all characterization tests, all ELS anodes were monitored. Monitoring ELS anodes allowed confirmation there was no crosstalk between anodes. Bench tests were performed prior to characterization, but this used regular signals. Laboratory test signals, due to their irregular nature, did highlight a special situation that was repaired before characterization could begin.

Laboratory characterization checks different instrument parameters to a standard set forth by the instrument specification (document number 02853-ELS_SPEC-01). For this, comparison to modeling of the ELS instrument was performed. Modeling of ELS was within tolerance error requirements and a combination of model results, characterization results, and calibration were used to determine the final ELS determination of flux values.

2.1 Theoretical Modeling

The ELS instrument is the electron half of a Tophat For All Species (TFAS). Sablik et al.¹ published TFAS characteristics, and specific ELS characteristics were determined from the TFAS design. ELS model results consist of many parameters that could not be checked in the laboratory, but acted as design aids in developing the ELS geometry.

The three main characteristics are the azimuthal, energy, and elevation responses. The azimuthal response was tuned so that electrons are focused in azimuth angle. The sharp azimuthal response is shown in Figure 1 and indicates a narrow azimuthal angle spread of the input electrons from a parallel electron beam.

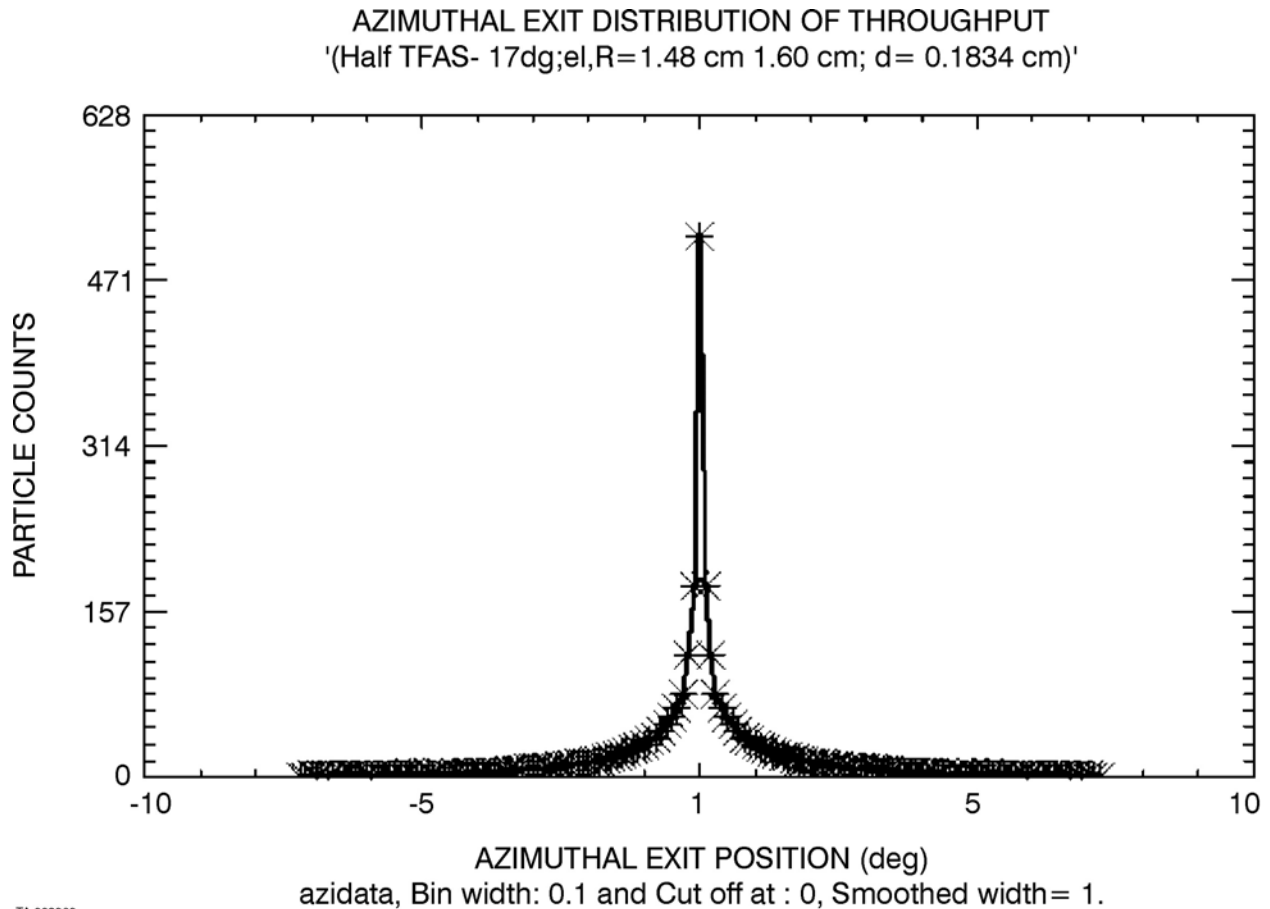


Figure 1. Theoretical ELS Azimuthal Response.

¹ Sablik, M. J., J. R. Scherrer, J. D. Winningham, R. A. Frahm, and T. Schrader, "TFAS (A Tophat For All Species): Design and Computer Optimization of a New Electrostatic Analyzer," IEEE Transactions on Geoscience and Remote Sensing, 28, 1034-1048, 1990.

Figure 2 shows the theoretical ELS energy response from electrons. The ELS energy response curve is characterized by its resolution parameter. For ELS, this is projected to be 8.24% ($\Delta E/E$). The modeling showed that the ELS geometric factor was $5.88 \times 10^{-4} \text{ cm}^2 \text{ sr}$. The instrument sensitivity is also generated from this curve. The sensitivity relates the energy of the source electrons to the voltage on the ELS deflection plate. This parameter determines how the instrument will step in voltage in order to obtain an energy spectrum.

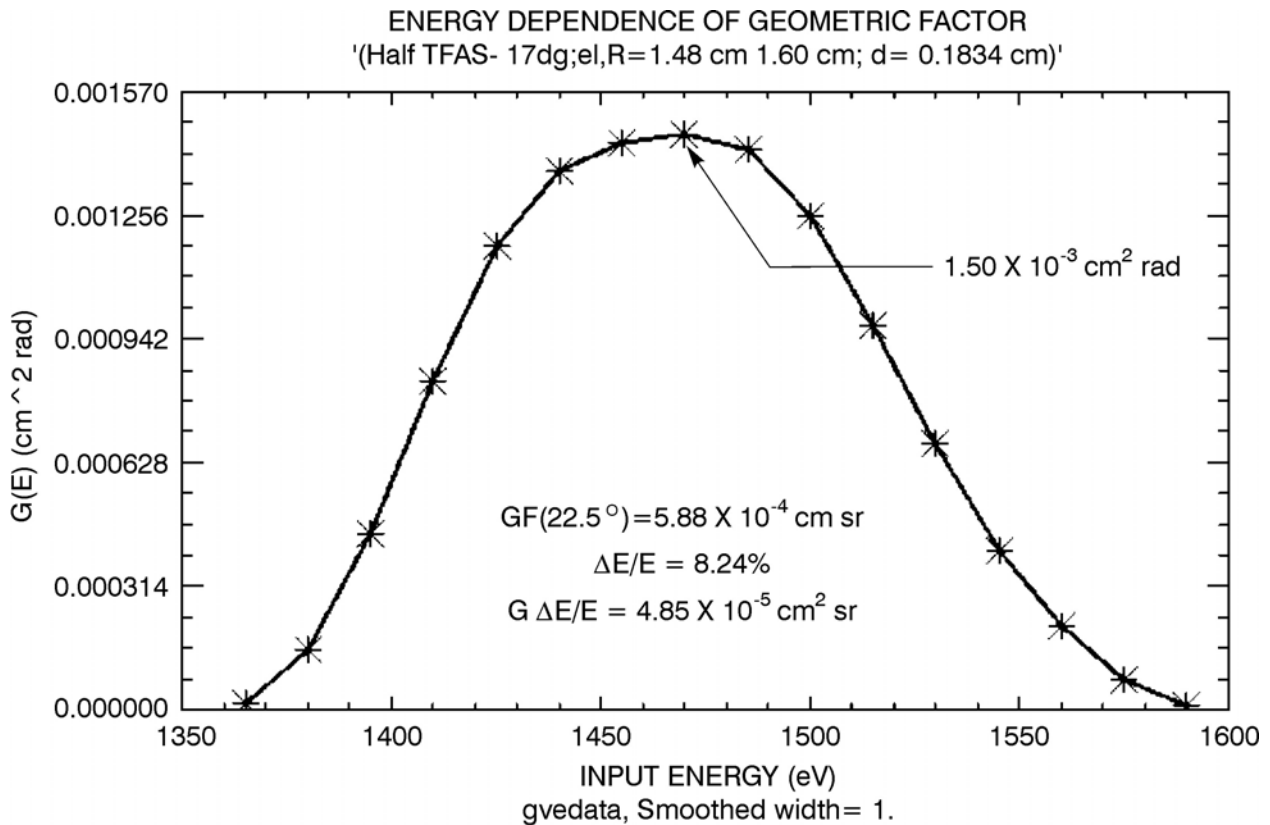


Figure 2. Theoretical ELS Energy Response.

In elevation angle, Figure 3 shows the ELS elevation response. The ELS modeling shows slight asymmetry in elevation angle. This fact has been taken into account when determining the geometric factor.

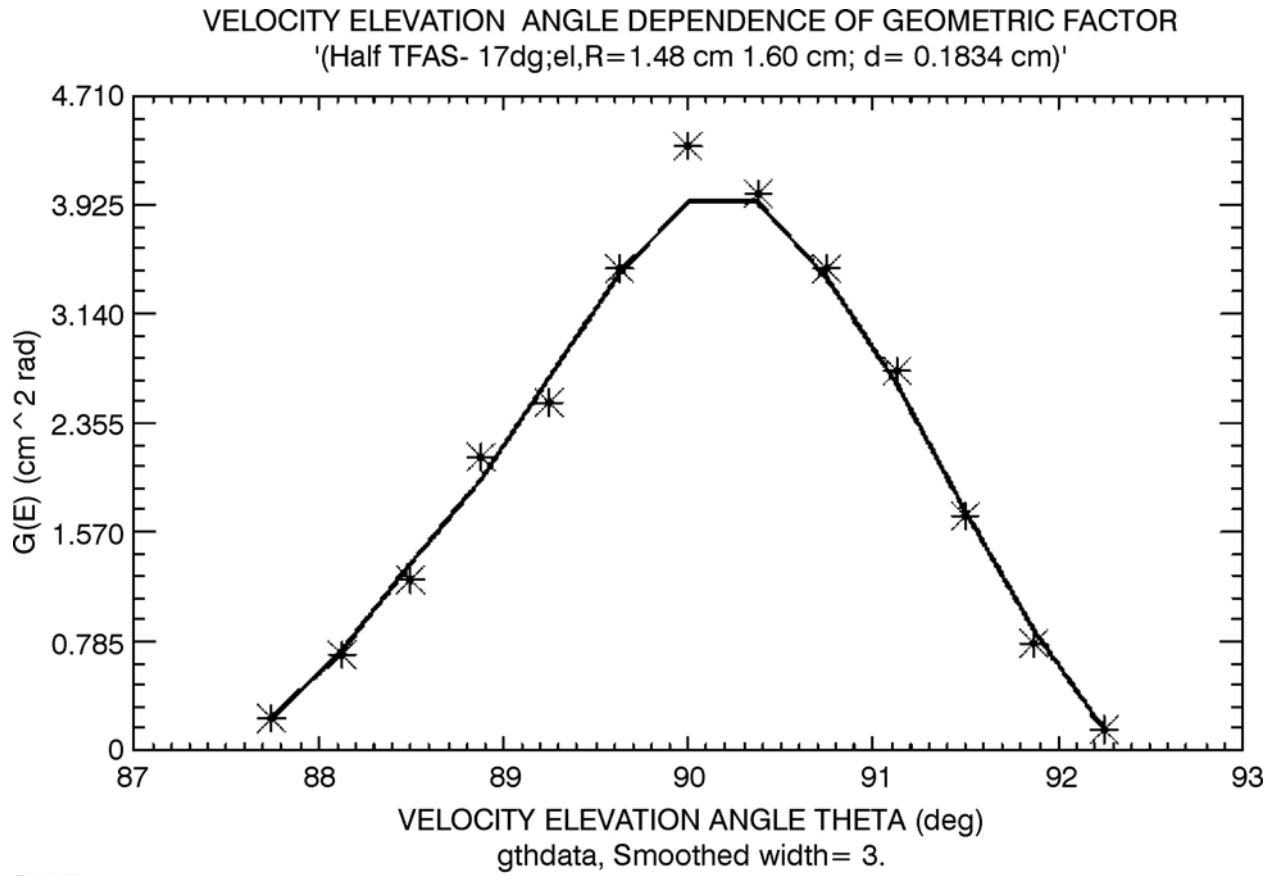


Figure 3. Theoretical ELS Elevation Response.

Although instrument characteristics may be well defined, the question remains as to whether the instrument can detect the expected electron plasma at Mars. ELS instrument characteristics were used in a simulation in order to determine if ELS will have the sensitivity and resolution required to perform measurements at Mars. An expected Mars electron distribution was used to simulate the Martian environment and the modeled ELS was used to generate simulated telemetry. The simulated telemetry was used with the instrument reconstruction formula in order to provide simulated measurements, proving that the modeled ELS is able to detect the expected electron plasma. These results are summarized in Figure 4. Characterization and calibration were performed in order to determine the differences between the "as built" ELS and the "modeled" ELS.

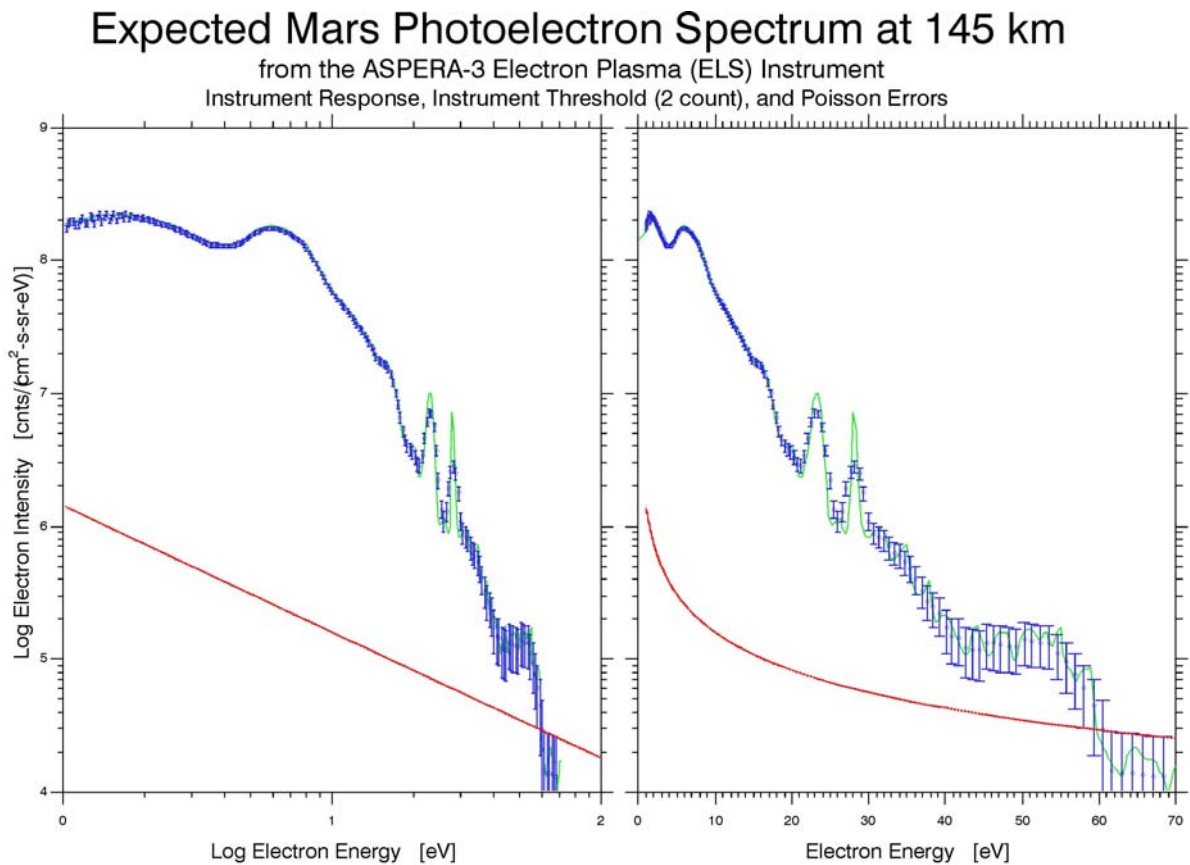


Figure 4. Simulated Response of Modeled ELS Measuring Expected Mars Ionospheric Electron Plasma.

2.2 ELS Characterization

ELS Characterization consists of four types of scans. Three scans are performed using a photoelectron gun while one uses a Ni-63 nuclear electron source. The three electron gun test types are MCP voltage scans, azimuth scans, and elevation scans. For the characterization, instrument count rates should be at manufacturers specification levels (about 30/s for ELS) for an accurate test. Count rates at higher values indicate that the instrument has not outgassed sufficiently. For this characterization, it is not necessary to be at the proper background levels.

These characterization tests can proceed as long as a signal of the electron beam is detectable. Proper outgassing is not achieved until the instrument has been in space for about a month.

2.2.1 ELS MCP Voltage Scans

An ELS MCP Voltage scan was performed in order to determine the operational voltage for the ELS MCP. If the MCP voltage is too low, an accurate representation of the instrument counts is not achieved; this means too many counts are below the instrument's counting threshold. If the MCP voltage is too high, an accurate representation of the instrument counts is again not achieved; there are too many self-generated noise pulses included in the MCP signal resulting in MCP noise being registered as counts. A balance between these is achieved by operating the instrument at or just above the lowest point at which the counts versus MCP voltage slope reduces. An example of an MCP scan from the ELS characterization is shown in Figure 5. From this curve, the ELS MCP voltage is about 2200V.

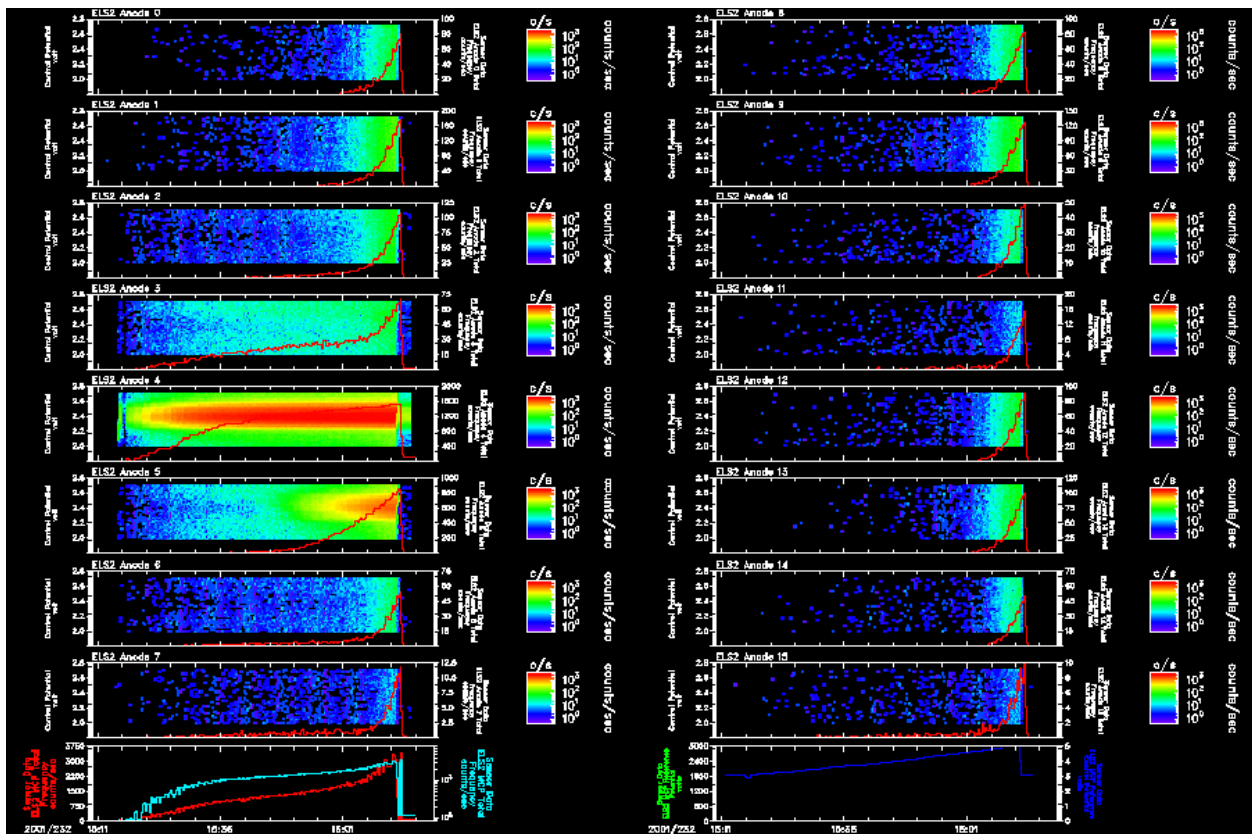


Figure 5. ELS MCP Voltage Scan using Electron Gun.

2.2.2 Azimuth Scans

The azimuth scan tests the azimuth acceptance, the relative intensity of each anode, the background of each anode, and the crosstalk between anodes. The MCP voltage is set to operational levels and the electron beam is centered at zero elevation. The detector is then revolved in azimuth. These results are shown in Figure 6 as a time progression of rotation. Here

it can be seen that when the beam is located in each sector, there is no crosstalk into other ELS sectors.

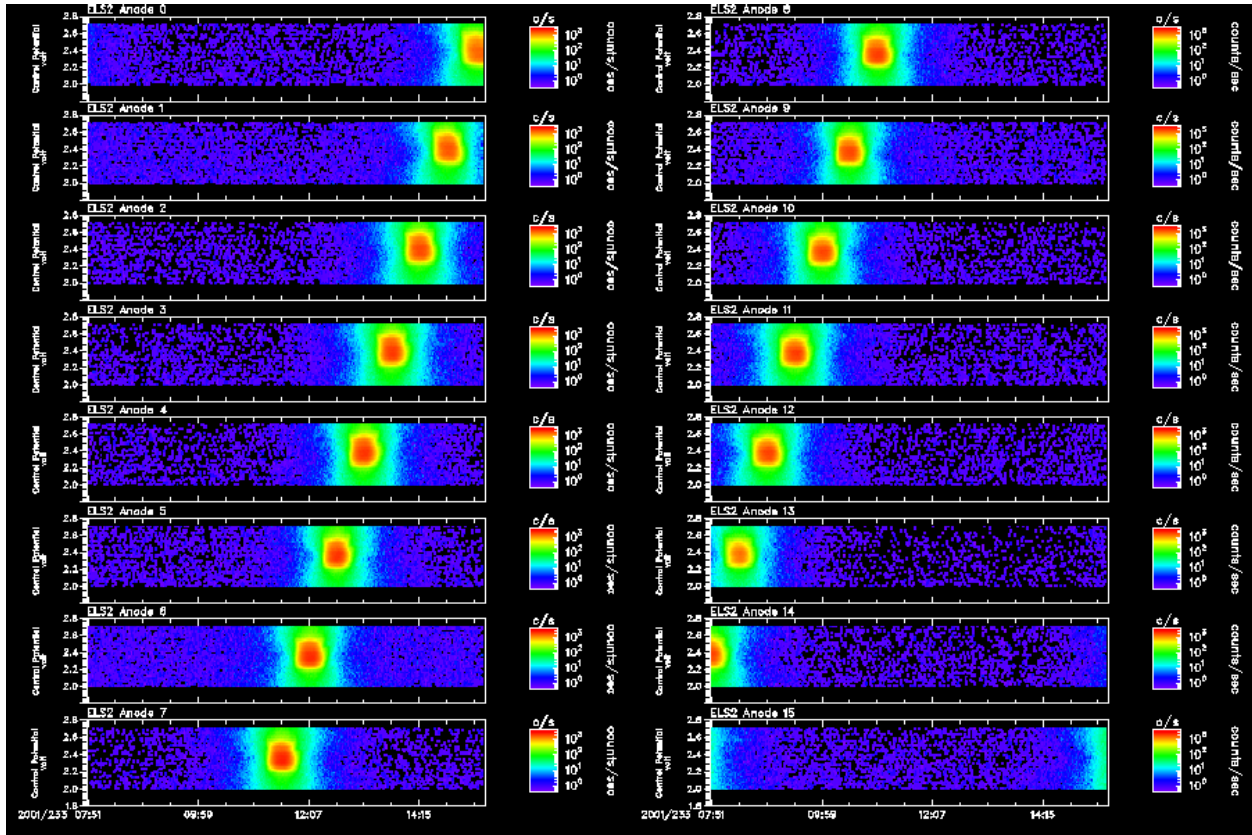


Figure 6. ELS Azimuth Scan using Electron Gun.

One observes that the vertical position of the beam does not change as the detector rotates in azimuth. This is an indication that the beam appears at a constant energy at all azimuths. The amount of signal in adjacent azimuth channels is more of an indicator of the spreading property of the electron beam than the instrument spread; however, the theoretical azimuthal distribution (Figure 1) does show that there is a non-zero azimuth value 7° away from the central peak. This indicates a low, non-zero value of flux should be observed at some azimuths away from the central peaks. This was observed during the characterization.

2.2.3 Elevation Scans

The elevation scans test the elevation acceptance, the relative intensity of each anode, the energy response of ELS, the background of each anode, and the crosstalk between anodes. Elevation scans are produced by a combination of scanning both the instrument elevation and the instrument deflection voltage at a constant beam energy. These scans are performed on each anode and the results are similar to those obtained from theory (see Figures 2 and 3). Elevation scan results are summarized in section 2.4.

2.3 Ni-63 Tests

A Nickel-63 (Ni-63) nuclear source was used to generate electrons. For each anode, the Ni-63 source was set at its azimuth center. The source was wider than the ELS elevation and covered the full elevation area. Plate voltages were scanned for 8 hours. These Ni-63 tests were used to normalize amplitudes as a function of energy. Ni-63 test results are summarized as relative efficiency tables in section 4.

2.4 Characterization Summary

Results of the ELS characterization provided values to compare against and verify theory. They produced a set of expected values for instrument characteristics and estimated anode variations. Sector voltage variations (Figure 7), sector resolution (Figure 8), and sector k-factor (Figure 9) showed slight variation from theory. These values should be regarded as only approximations allowing for estimates before going into a calibration facility. The characterization facility did not have the resolution and accuracy required to perform the ELS calibration. Thus, ELS calibration was performed at Mullard Space Science Laboratory (MSSL).

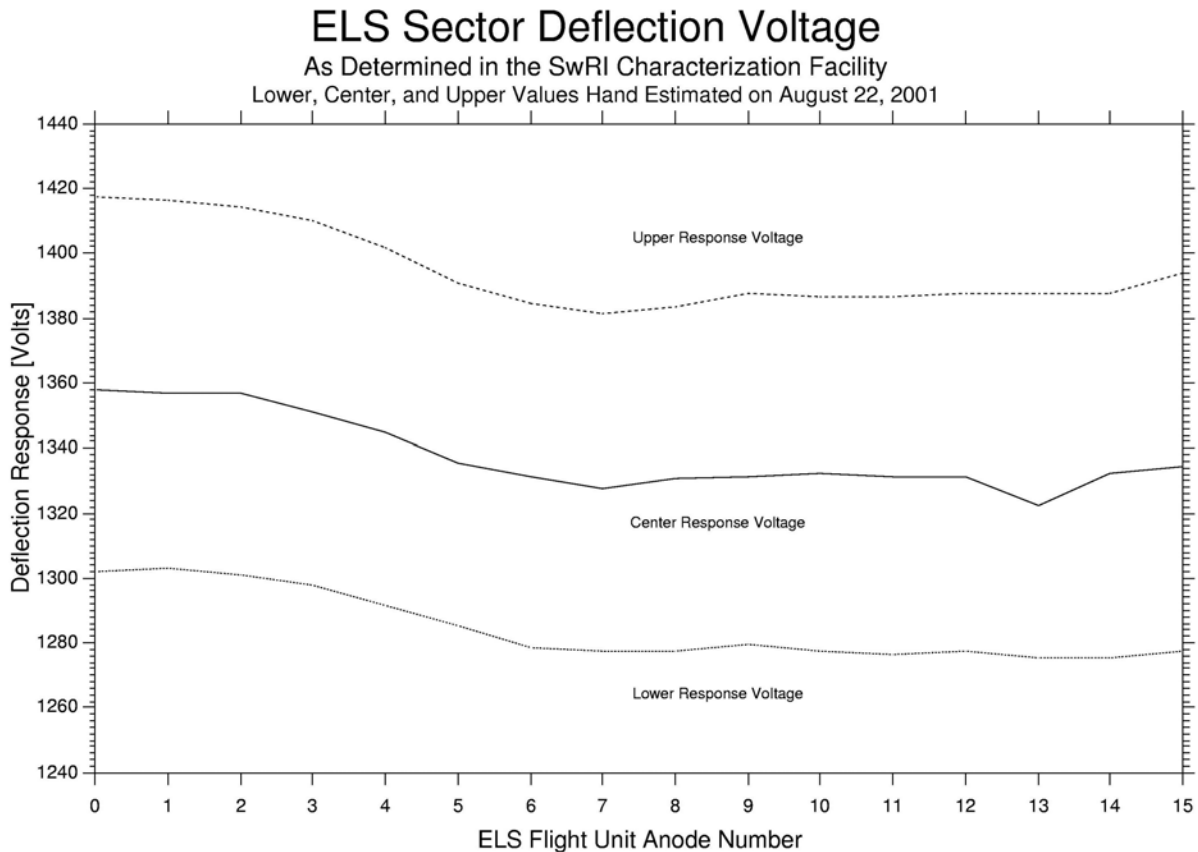


Figure 7. ELS Sector Deflection Voltage Variation Showing Width of the Measured Voltage Response.

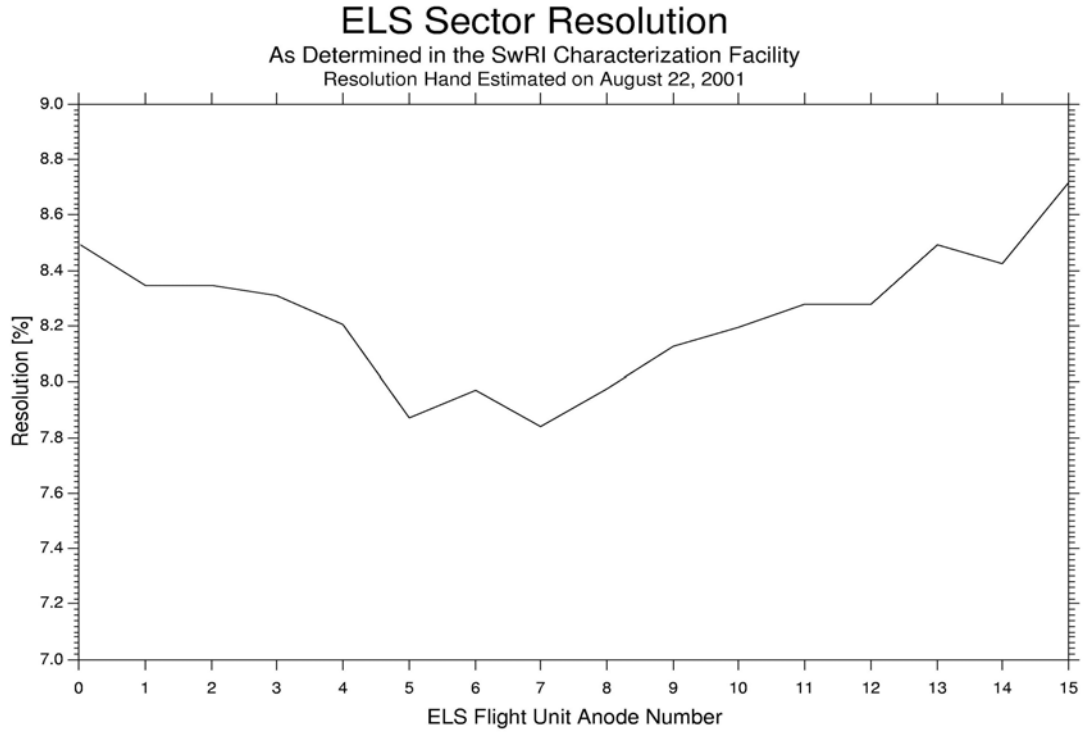


Figure 8. ELS Sector Resolution Determined from the Energy Response.

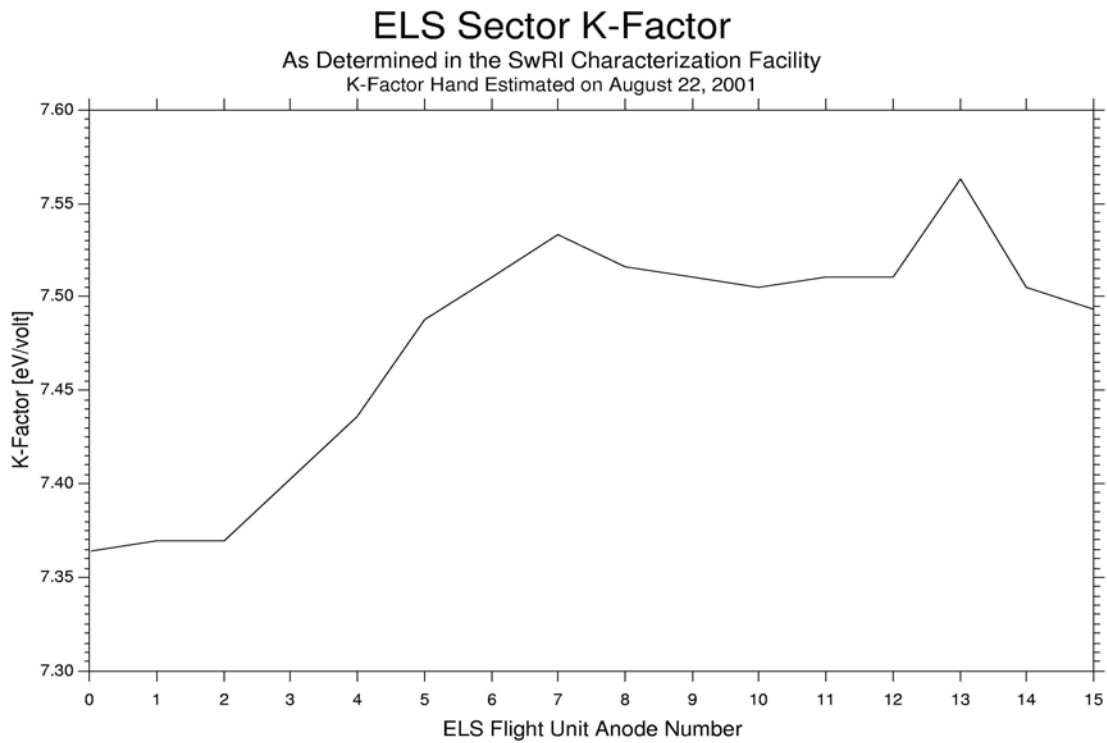


Figure 9. ELS Sector K-Factor Determined from the Energy Response.

3. MSSL Calibration of ELS

SwRI facilities did not have the measurement resolution required for ELS calibration. ELS exceeded the pointing and position resolution requirements of the facility at SwRI. In addition, the photoelectron gun used in SwRI's calibration facility is not able to maintain flux at low beam energies, and the facility is not magnetically shielded. Both the physics of photon interaction and electron-magnetic field interaction prevent maintaining the flux at the low energies required for ELS measurement. In order to achieve the needed calibration requirements, the ELS calibration was performed at MSSL. See DOCUMENT: MSSL/MEX/017, Dated Mar 18th 2002.

4. ELS Calibration

ELS calibration parameters are refined in several stages. The first stage encompasses the initial SwRI results of Characterization. The MSSL Calibration results refine these values in the second stage. The third stage applies science offsets to the parameters for each sector. The fourth stage updates the MSSL calibration from refined fitting to the MSSL calibration, relative sector variations from SwRI Ni-63 data and inclusion of physical blockage parameters. A fifth stage will include the absolute efficiency curve, but a scientifically valid estimation to use for all sectors is 0.95.

Development of ELS Flight Unit Calibration Tables

- Determine MCP Transparency: $M_T = 58\%$ (quoted by manufacture)
- Determine Grid Transparency: $G_T = 81.0\% \pm 1.8\%$ (see SwRI Document ES-SGT-10-03561)
- Determine Active Anode Area Ratio: $A_A = 0.87 \pm 0.01$ (Manufactured / Theory)
- Determine ELS Sensitivity: $S_E = \frac{E_c}{V_p}$ (also called K-factor) - see Table
- Determine ELS Resolution: $R_E = \frac{\Delta E}{E_c}$ - see Table
- Determine Scaling Factors for Each ELS Anode: S_F - see Procedure* (below) and Table
- Determine ELS MCP Efficiency: ϵ
 - determine Ni-63 efficiency difference ϵ_R (relative) - see Table
 - determine Bordoni efficiency ϵ_A (absolute) - Estimated ~0.95

True Differential Number Flux per Energy Channel per Anode:
$$j = \frac{\text{counts} \cdot S_F}{\text{PGF} \cdot M_T \cdot G_T \cdot A_A \cdot \Delta t \cdot R_E \cdot E_c \cdot (\epsilon_A / \epsilon_R)}$$

— where PGF = Physical Geometric Factor for an ELS Anode, $5.88 \times 10^{-4} \text{ cm}^2 \text{ sr}$
 Δt = Accumulation Time for an ELS Energy Step, $2.8125 \times 10^{-2} \text{ sec}$

**Procedure Dr. J. David Winningham used to generate Science Scaling Factors (S_F) for ELS:*

It was recognized that the position for mounting the ELS on the Mars Express spacecraft caused some of its sectors to be partially blocked. In response, a set of Science Scaling Factors for ELS was specified for the purpose of describing an external influence (e.g. the blocking of sectors by the spacecraft) on ELS. Initially, the Science Scaling Factors were defined to be fractional amounts of electron flux transmission reaching the instrument; a value of 1.0 meant total transmission (no external blockage of the FOV by the spacecraft) and a value of 0.0 meant that the sector transmission is totally blocked by the spacecraft.

The ELS Science Scaling Factors were defined by the ELS PI, Dr. J. David Winningham, in a series of two analysis periods. The initial factors were set to 1.0 for each of the 16 ELS sectors, indicating 100% flux transmission. Adjustments to the ELS Science Scaling Factors acted to multiply on the previous set of ELS Science Scaling Factors which were in use at that time.

The first time period that Dr. Winningham examined was 9 July 2003, when the Mars Express spacecraft was in the solar wind. From 1900 UT through 2000 UT, Mars Express changed pointing direction. Dr. Winningham examined the ELS spectra from each sector and matched their flux amplitude with the corresponding ELS sector based on symmetry about the radial Sun vector. This determined the first set of ELS Science Scaling Factors.

In mid-July of 2004, the second set of ELS Science Scaling Factors was determined by Dr. Winningham using a similar method. At this time, the Mars Express spacecraft was orbiting Mars. Two types of spectra were examined, solar wind spectra and tail spectra. The solar wind spectra were examined first and provided multipliers on the ELS Science Scaling Factors. These time periods were from 4 July 2004 (02:28:00) and 21 May 2004 (19:40:00). The tail spectra examined provided multipliers on those determined from the solar wind spectra and were from 20 May 2004 (01:20:57, 01:21:57, 01:22:57, 01:22:39, 01:23:07, 01:23:48, 01:24:28, 01:25:04, 01:26:04, 01:20:55) and 13 June 2004 (23:28:02). During this process, contours of energy flux were examined and the flux amplitudes at the energy peaks were selected to be identical. Adjustments were chosen to tweak amplitudes such that the flux values at the peak for each sector were the same.

After Dr. Winningham's analysis, some of the ELS Science Scaling Factors exceeded values of 1.0 and others were amplitudes not as expected. This is because he did a scientific evaluation of the entire distribution, matching and adjusting the amplitudes of each sector in energy flux at the distribution peak around the observation plane.

During both time periods, the ASPERA-3 scanner was in its launch position. In the launch position, ELS sectors 0, 14, and 15 completely overlook the spacecraft, sector 12 partly overlooks the spacecraft, sector 13 views the Mars Express solar array rotating arm, and sector 1 contains a sun sensor in its FOV. The ASPERA-3 scanner remained in the launch position until its activation 20 January 2006.

ELS Flight Unit Calibration Table

ELS Anode	Sensitivity $S_E = \frac{E_c}{V_p}$	Resolution $R_E = \frac{\Delta E}{E_c}$	Scaling Factor S_F	Relative Efficiency ϵ_R
0	7.167	8.653e-2	2.632867	$2141859e-6 + -6024497e-9 * V_c + 1794353e-11 * V_c^{**2} + -2796459e-14 * V_c^{**3} + 2543964e-17 * V_c^{**4} + -1395010e-20 * V_c^{**5} + 4532808e-24 * V_c^{**6} + -8024142e-28 * V_c^{**7} + 5954283e-32 * V_c^{**8}$
1	7.152	8.394e-2	1.000000	$1660858e-6 + -6522166e-9 * V_c + 3691054e-11 * V_c^{**2} + -1073737e-13 * V_c^{**3} + 1839852e-16 * V_c^{**4} + -1977613e-19 * V_c^{**5} + 1369280e-22 * V_c^{**6} + -6096699e-26 * V_c^{**7} + 1685387e-29 * V_c^{**8} + -2630885e-33 * V_c^{**9} + 1771363e-37 * V_c^{**10}$
2	7.141	8.331e-2	0.635386	$2021935e-6 + -5955053e-9 * V_c + 1878866e-11 * V_c^{**2} + -3736588e-14 * V_c^{**3} + 5172668e-17 * V_c^{**4} + -5034701e-20 * V_c^{**5} + 3363807e-23 * V_c^{**6} + -1488898e-26 * V_c^{**7} + 4137518e-30 * V_c^{**8} + -6504663e-34 * V_c^{**9} + 4399947e-38 * V_c^{**10}$
3	7.165	8.579e-2	0.712443	$1659460e-6 + -4954925e-9 * V_c + 1526991e-11 * V_c^{**2} + -2516840e-14 * V_c^{**3} + 2433297e-17 * V_c^{**4} + -1420192e-20 * V_c^{**5} + 4915142e-24 * V_c^{**6} + -9275283e-28 * V_c^{**7} + 7345382e-32 * V_c^{**8}$
4	7.188	8.124e-2	0.810931	$1731412e-6 + -5380326e-9 * V_c + 1709947e-11 * V_c^{**2} + -2884332e-14 * V_c^{**3} + 2826155e-17 * V_c^{**4} + -1658431e-20 * V_c^{**5} + 5735419e-24 * V_c^{**6} + -1076440e-27 * V_c^{**7} + 8447731e-32 * V_c^{**8}$
5	7.625	8.480e-2	0.896400	$1811691e-6 + -5230411e-9 * V_c + 1584896e-11 * V_c^{**2} + -2629686e-14 * V_c^{**3} + 2573125e-17 * V_c^{**4} + -1519547e-20 * V_c^{**5} + 5306596e-24 * V_c^{**6} + -1006748e-27 * V_c^{**7} + 7984914e-32 * V_c^{**8}$
6	7.262	8.194e-2	1.370552	$9984187e-7 + 2018039e-10 * V_c + -3170439e-12 * V_c^{**2} + 1589455e-14 * V_c^{**3} + -3484247e-17 * V_c^{**4} + 4156025e-20 * V_c^{**5} + -2951669e-23 * V_c^{**6} + 1283619e-26 * V_c^{**7} + -3351854e-30 * V_c^{**8} + 4821632e-34 * V_c^{**9} + -2933104e-38 * V_c^{**10}$
7	7.266	7.890e-2	0.928571	$1593066e-6 + -2964337e-9 * V_c + 3217016e-12 * V_c^{**2} + 9241350e-15 * V_c^{**3} + -3138800e-17 * V_c^{**4} + 4137379e-20 * V_c^{**5} + -3044785e-23 * V_c^{**6} + 1346434e-26 * V_c^{**7} + -3552330e-30 * V_c^{**8} + 5151235e-34 * V_c^{**9} + -3156380e-38 * V_c^{**10}$
8	7.275	7.812e-2	0.665921	$2097414e-6 + -3125151e-9 * V_c + -4329302e-12 * V_c^{**2} + 4317461e-14 * V_c^{**3} + -9923385e-17 * V_c^{**4} + 1177737e-19 * V_c^{**5} + -8280358e-23 * V_c^{**6} + 3573841e-26 * V_c^{**7} + -9293869e-30 * V_c^{**8} + 1335333e-33 * V_c^{**9} + -8131189e-38 * V_c^{**10}$
9	7.254	8.094e-2	1.000000	$2062909e-6 + -4885969e-9 * V_c + 1427184e-11 * V_c^{**2} + -2260352e-14 * V_c^{**3} + 2111094e-17 * V_c^{**4} + -1194770e-20 * V_c^{**5} + 4024074e-24 * V_c^{**6} + -7416131e-28 * V_c^{**7} + 5754756e-32 * V_c^{**8}$
10	7.262	8.095e-2	0.807453	$2180664e-6 + -6296202e-9 * V_c + 1891070e-11 * V_c^{**2} + -3064724e-14 * V_c^{**3} + 2948811e-17 * V_c^{**4} + -1724577e-20 * V_c^{**5} + 5997964e-24 * V_c^{**6} + -1138182e-27 * V_c^{**7} + 9060635e-32 * V_c^{**8}$
11	7.255	8.346e-2	1.000000	$1603139e-6 + -8534362e-10 * V_c + -8667849e-12 * V_c^{**2} + 4394307e-14 * V_c^{**3} + -8845054e-17 * V_c^{**4} + 9830094e-20 * V_c^{**5} + -6619258e-23 * V_c^{**6} + 2766078e-26 * V_c^{**7} + -7009821e-30 * V_c^{**8} + 9858768e-34 * V_c^{**9} + -5896570e-38 * V_c^{**10}$
12	7.255	8.297e-2	0.988789	$2026128e-6 + -3624418e-9 * V_c + 1755093e-12 * V_c^{**2} + 2385497e-14 * V_c^{**3} + -6688306e-17 * V_c^{**4} + 8554336e-20 * V_c^{**5} + -6280654e-23 * V_c^{**6} + 2795381e-26 * V_c^{**7} + -7448619e-30 * V_c^{**8} + 1092352e-33 * V_c^{**9} + -6770721e-38 * V_c^{**10}$
13	7.271	7.353e-2	1.461922	$4264294e-6 + -2121222e-8 * V_c + 8360316e-11 * V_c^{**2} + -1760020e-13 * V_c^{**3} + 2193857e-16 * V_c^{**4} + -1690439e-19 * V_c^{**5} + 8124086e-23 * V_c^{**6} + -2368735e-26 * V_c^{**7} + 3831171e-30 * V_c^{**8} + -2635711e-34 * V_c^{**9}$
14	7.253	7.396e-2	0.928571	$1871975e-6 + -2714091e-9 * V_c + -1640371e-12 * V_c^{**2} + 3116431e-14 * V_c^{**3} + -7626180e-17 * V_c^{**4} + 9286905e-20 * V_c^{**5} + -6636238e-23 * V_c^{**6} + 2903883e-26 * V_c^{**7} + -7657761e-30 * V_c^{**8} + 1117466e-33 * V_c^{**9} + -6928145e-38 * V_c^{**10}$
15	7.188	8.843e-2	2.146711	$1714980e-6 + -7089766e-9 * V_c + 3259217e-11 * V_c^{**2} + -8410868e-14 * V_c^{**3} + 1347052e-16 * V_c^{**4} + -1391524e-19 * V_c^{**5} + 9397261e-23 * V_c^{**6} + -4114030e-26 * V_c^{**7} + 1123482e-29 * V_c^{**8} + -1737531e-33 * V_c^{**9} + 1161350e-37 * V_c^{**10}$

Note that V_c is the voltage across the deflection plates when ELS measures energy E_c

This page intentionally left blank.

This page intentionally left blank.

Mars Express ASPERA ELS

MULLARD SPACE SCIENCE LABORATORY

UNIVERSITY COLLEGE LONDON

Author: Dave Linder

Mars Express ASPERA ELS Flight Unit Calibration Report Volume 1: Experimental Set-up, Instrument Power-On, Deadtime Tests and Beam Characterisation

DOCUMENT: MSSL/MEX/017

Mar 18th 2002

1. Installation

The ELS Flight Unit was installed in the calibration chamber on November 23rd 2001. Photographs of the set-up inside the chamber are shown in Figures 1.1 and 1.2. The configuration is as for previous tests at MSSL but with a new line driver system inserted between ELS and the counters outside the chamber. The line drivers are inside the grey box below ELS. A channeltron for independent monitoring of the beam intensity is mounted adjacent to the ELS aperture on the left.

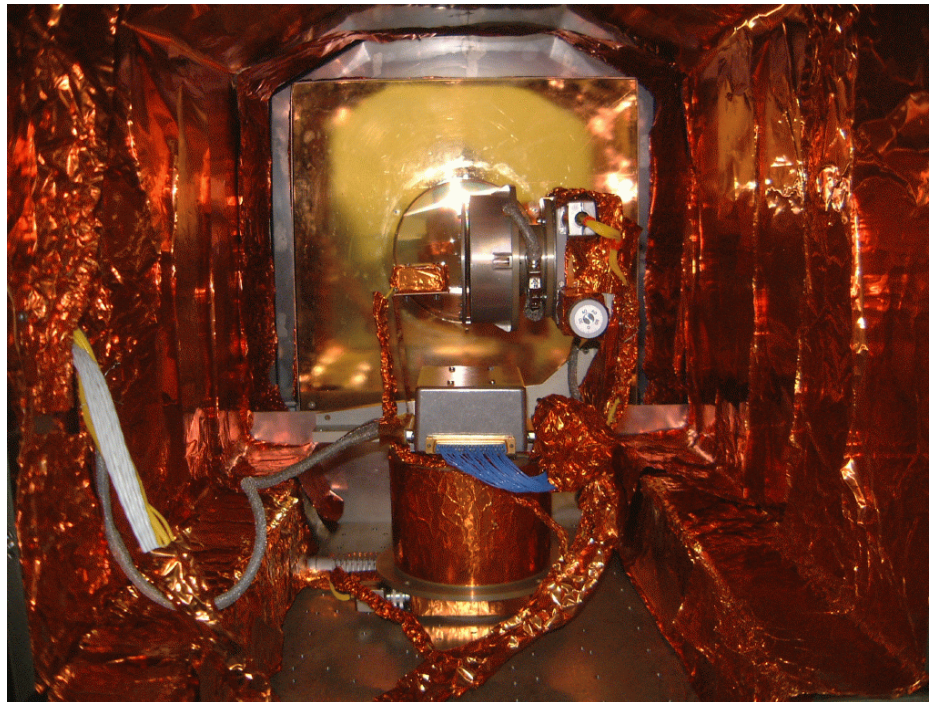


Figure 1.1: ELS FU mounted inside the MSSL calibration chamber on November 23rd 2001.

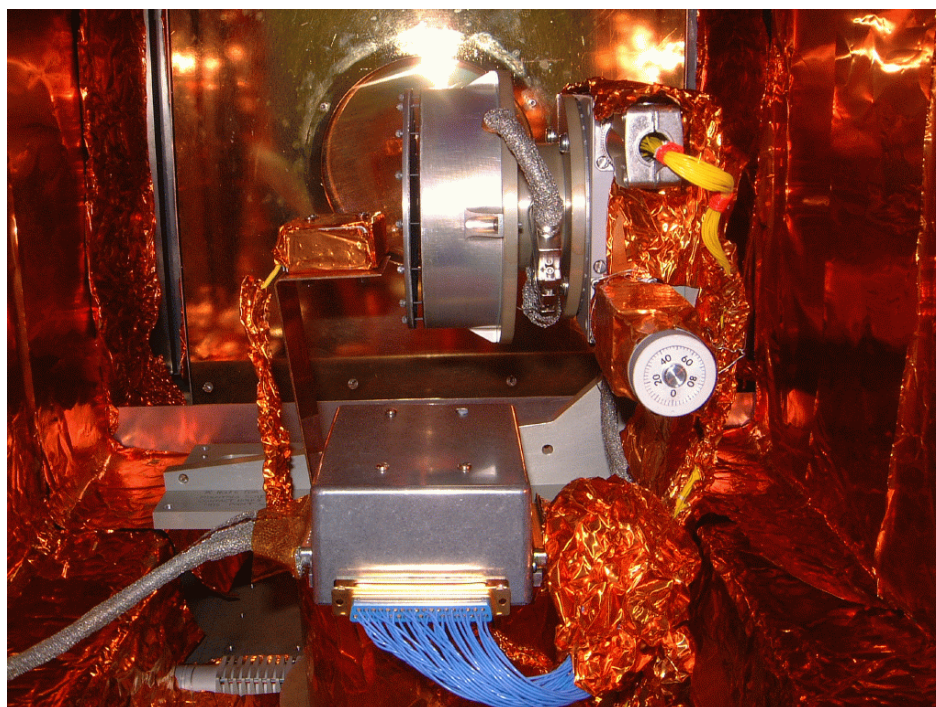
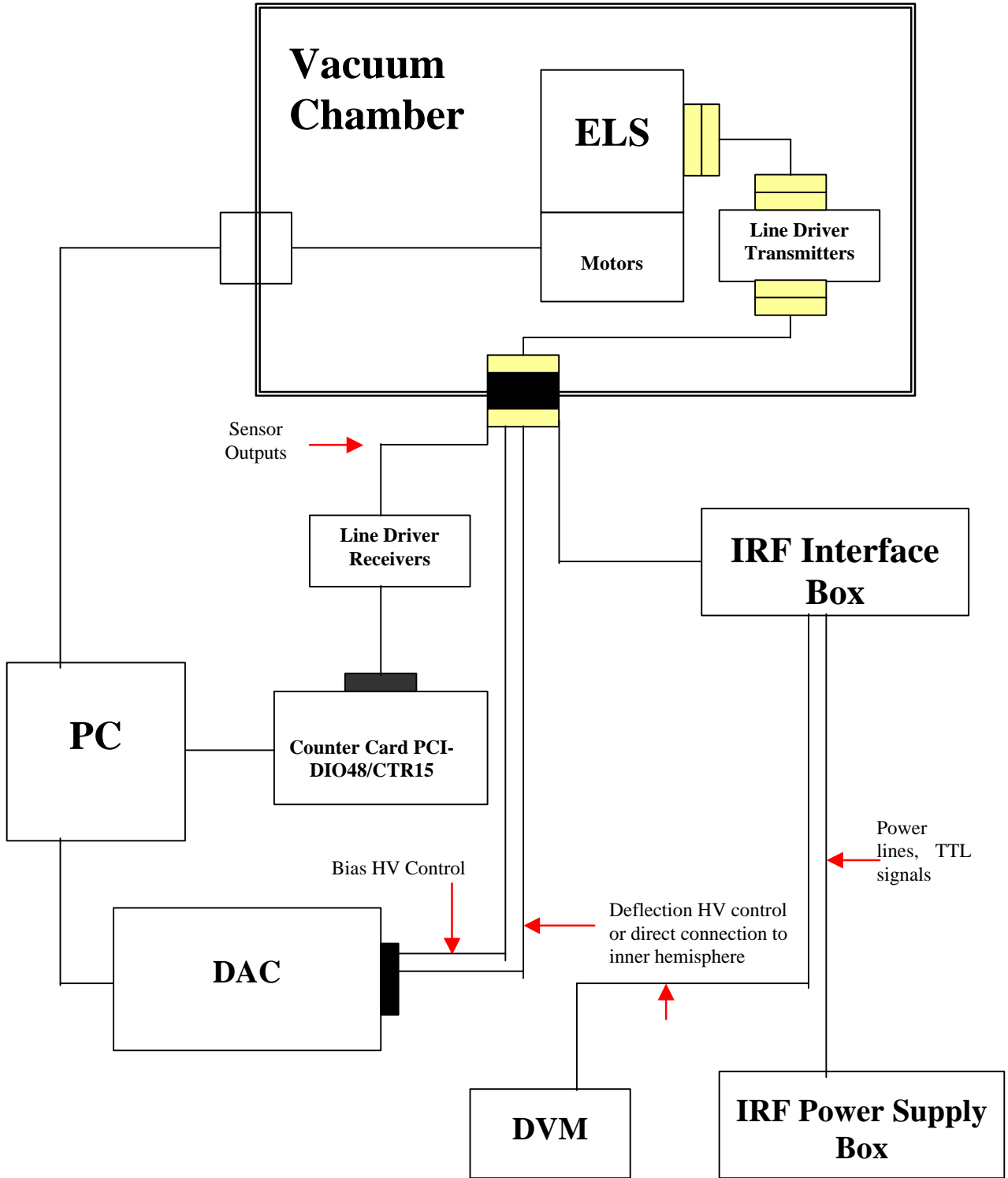


Figure 1.2: ELS FU mounted inside the MSSL calibration chamber on November 23rd 2001.

Figure 1.3: Block diagram of the calibration configuration



A block diagram demonstrating the set-up is shown in Figure 1.3. A more detailed diagram of the line driver configuration is shown in Figure 1.4.

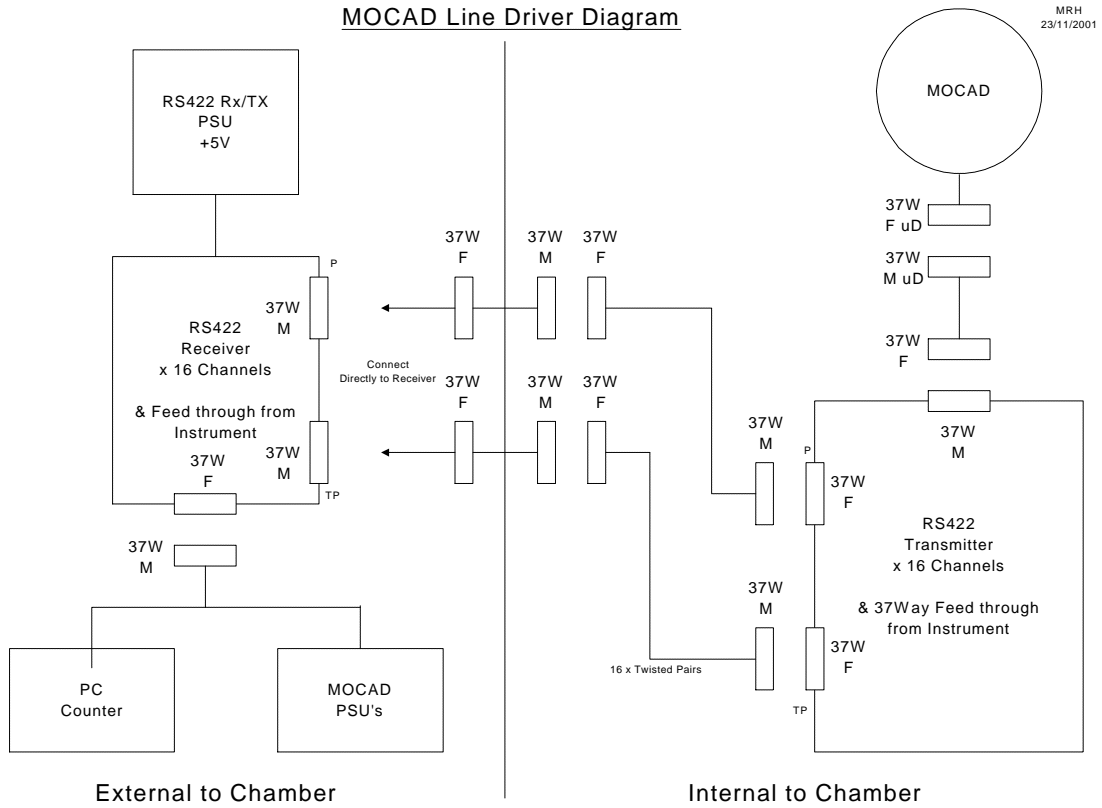


Figure 1.4: Block diagram of the MSSL line drivers

2. Power-up December 3rd 2001

ELS was powered on according to the files described in Tables 2.1 and 2.2.

Filename	AF2100B.PAC/PDT
Date	Dec 3 rd 2001
Beam Energy (eV)	Beam off
MCP Level (DAC Volts)	2.6 / 3.5 / step 0.1
MCP Level (Actual Volts)	1200 / 2100 / step 60
Sweep Level (DAC Volts)	0
Acquisition Length (seconds)	10
No. of Acquisitions at each level	15

Table 2.1: Power-on file AF2100B

Filename	AF2340B.PAC/PDT
Date	Dec 3 rd 2001
Beam Energy (eV)	Beam off
MCP Level (DAC Volts)	3.6 / 3.9 / step 0.1
MCP Level (Actual Volts)	2160 / 2340 / step 60
Sweep Level (DAC Volts)	0
Acquisition Length (seconds)	10
No. of Acquisitions at each level	15

Table 2.2: Power-on file AF2340B

The background count-rates recorded on ELS during the power-up are presented in Figure 2.1.

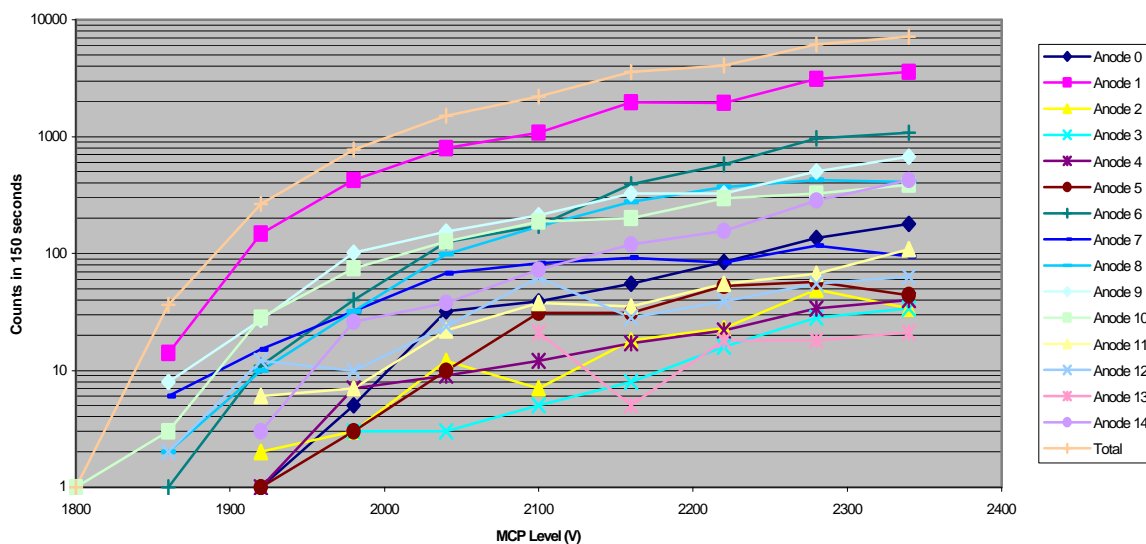


Figure 2.1: ELS background count-rates during power-up on December 3rd 2001

The power-up procedure for all subsequent turn-ons is given in Appendix A.

3. Power-up December 4th 2001

The format of the power-up file on December 4th 2001 is shown in Tables 3.1 to 3.3.

Filename	AFON235D.PAC/PDT
Date	Dec 4 th 2001
Beam Energy (eV)	Beam off
MCP Level (DAC Volts)	0 / 3.5 / step 0.5
MCP Level (Actual Volts)	0 / 2100 / step 300
Sweep Level (DAC Volts)	0
Acquisition Length (seconds)	3
No. of Acquisitions at each level	5

Table 2.2: Power-on file AFON235D.PAC Part 1

Filename	AFON235D.PAC/PDT
Date	Dec 4 th 2001
Beam Energy (eV)	Beam off
MCP Level (DAC Volts)	3.6 / 3.9 / step 0.1
MCP Level (Actual Volts)	2160 / 2340 / step 60
Sweep Level (DAC Volts)	0
Acquisition Length (seconds)	10
No. of Acquisitions at each level	5

Table 2.2: Power-on file AFON235D.PAC Part 2

Filename	AFON235D.PAC/PDT
Date	Dec 4 th 2001
Beam Energy (eV)	Beam off
MCP Level (DAC Volts)	3.93
MCP Level (Actual Volts)	2358
Sweep Level (DAC Volts)	0
Acquisition Length (seconds)	10
No. of Acquisitions at each level	5

Table 2.2: Power-on file AFON235D.PAC Part 3

All subsequent power-ups used the same file format e.g. AFON235E.PAC on December 5th 2001. The background count-rates recorded on ELS during the power-up on December 4th are presented in Figure 3.1.

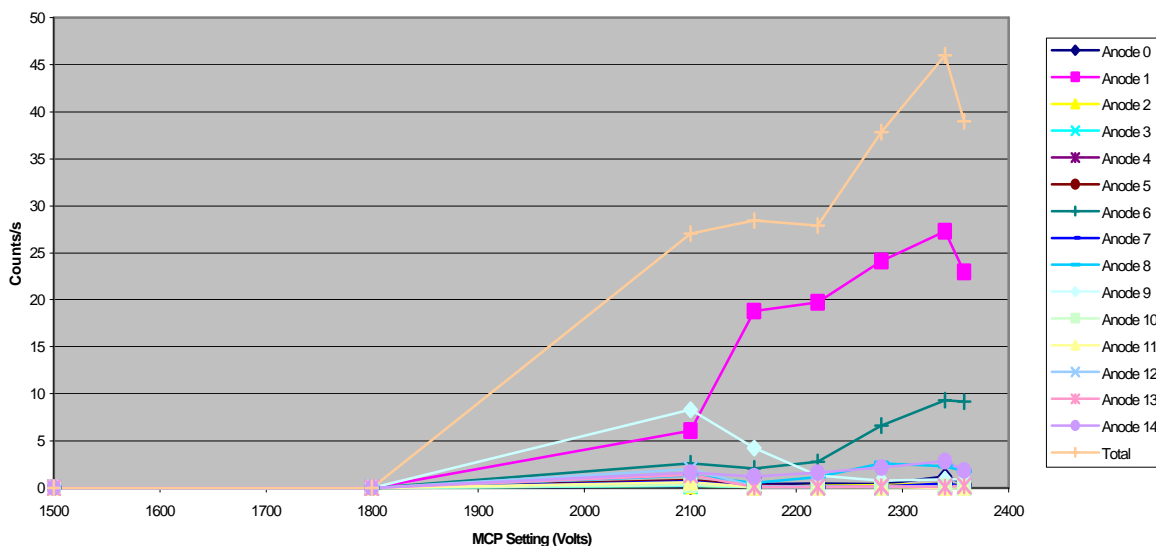


Figure 3.1: ELS background count-rates during power-up on December 4th 2001

4. Power-up December 5th 2001

The power-up file was AFON235E.PAC. The background count-rates recorded on ELS during the power-up are presented in Figure 4.1.

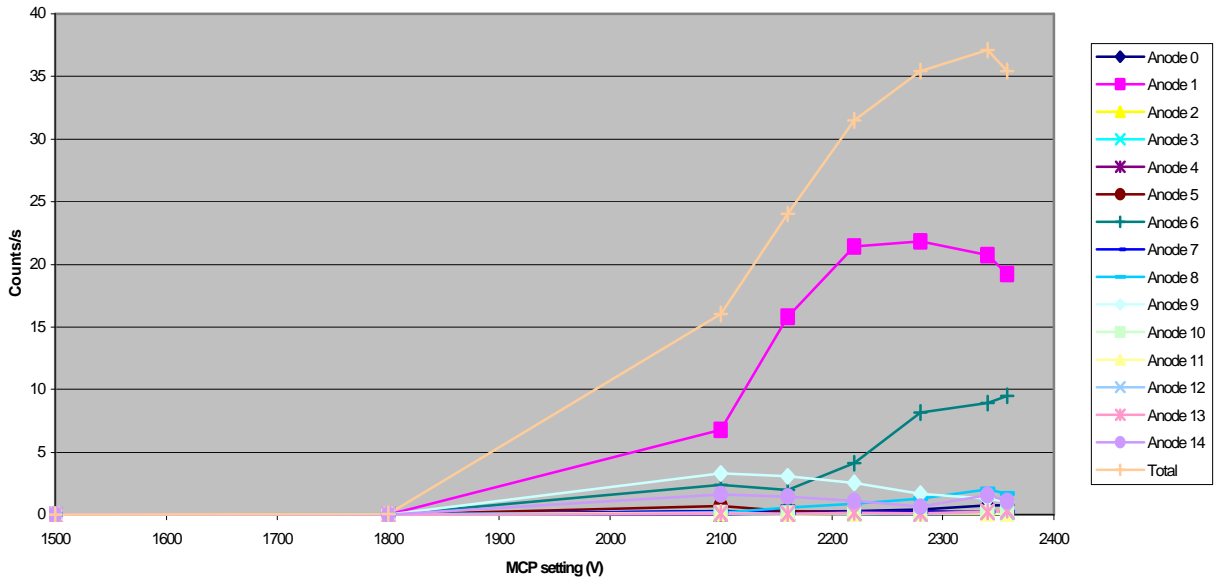


Figure 4.1: ELS background count-rates during power-up on December 5th 2001

5. Power-up December 6th 2001

The power-up file was AFON235F.PAC. The background count-rates recorded on ELS during the power-up are presented in Figure 5.1.

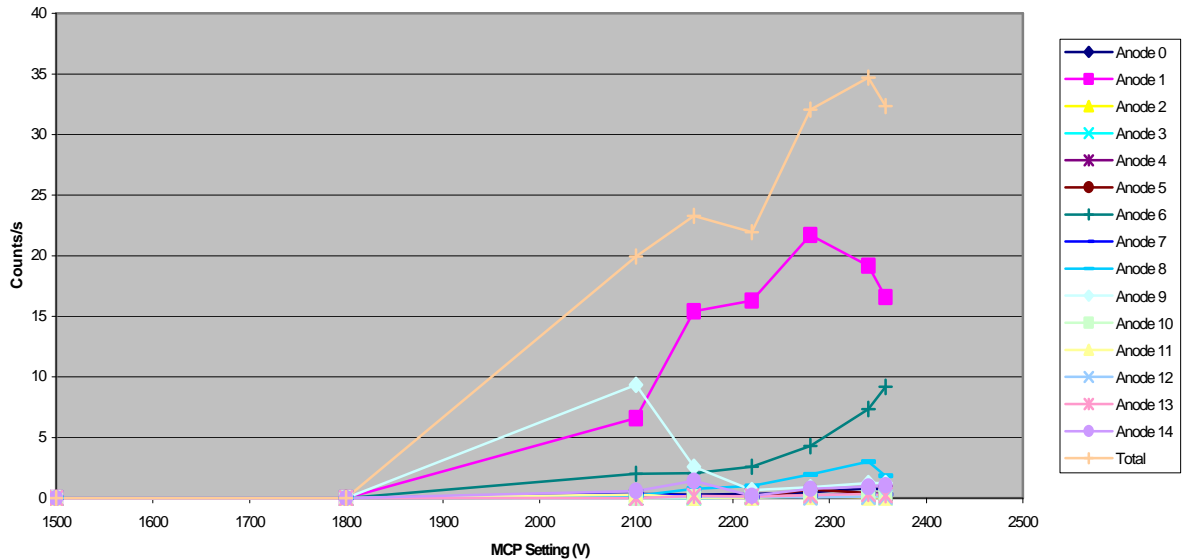


Figure 5.1: ELS background count-rates during power-up on December 6th 2001

6. Power-up December 7th 2001

The power-up file was AFON235G.PAC. The background count-rates recorded on ELS during the power-up are presented in Figure 6.1.

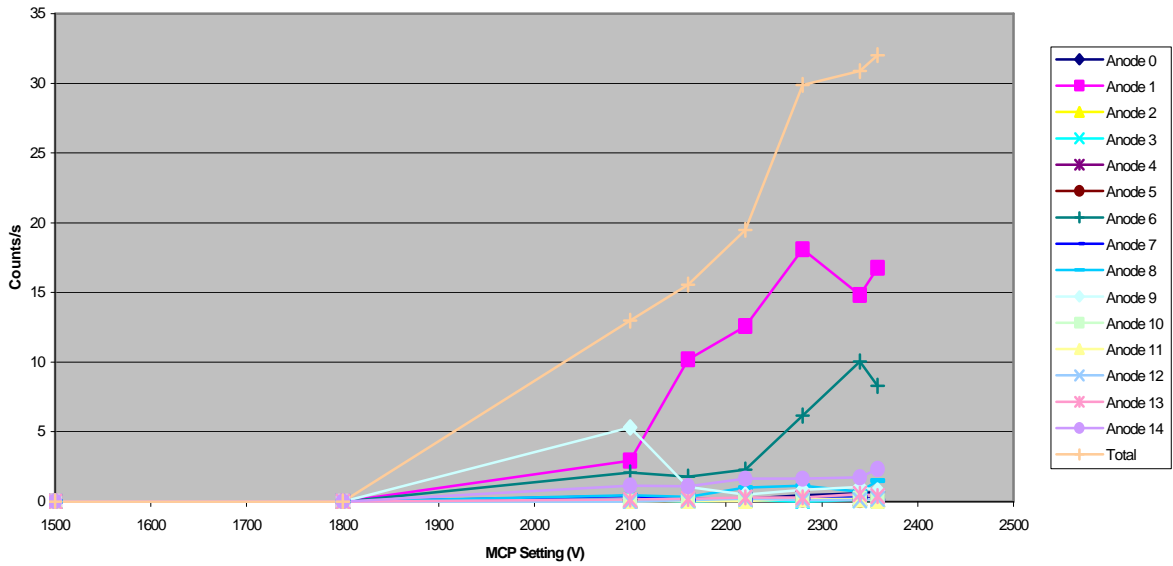


Figure 6.1: ELS background count-rates during power-up on December 7th 2001

7. Power-up December 10th 2001

The power-up file was AFON235H.PAC. The background count-rates recorded on ELS during the power-up are presented in Figure 7.1.

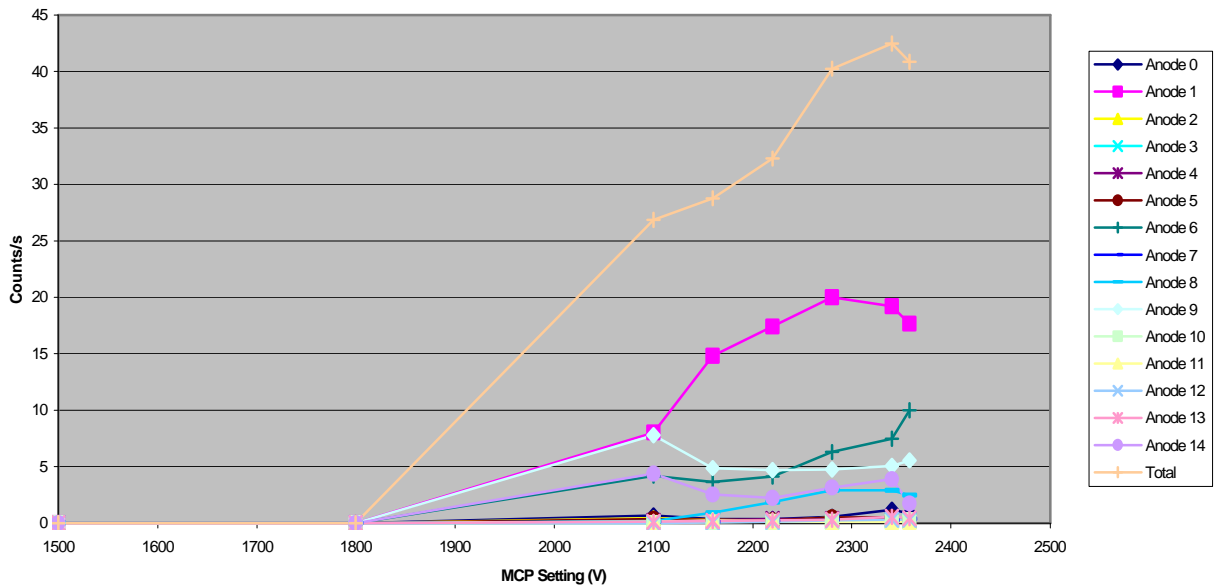


Figure 7.1: ELS background count-rates during power-up on December 10th 2001

8. Power-up December 17th 2001

The power-up file was AFON235J.PAC. The background count-rates recorded on ELS during the power-up are presented in Figure 8.1.

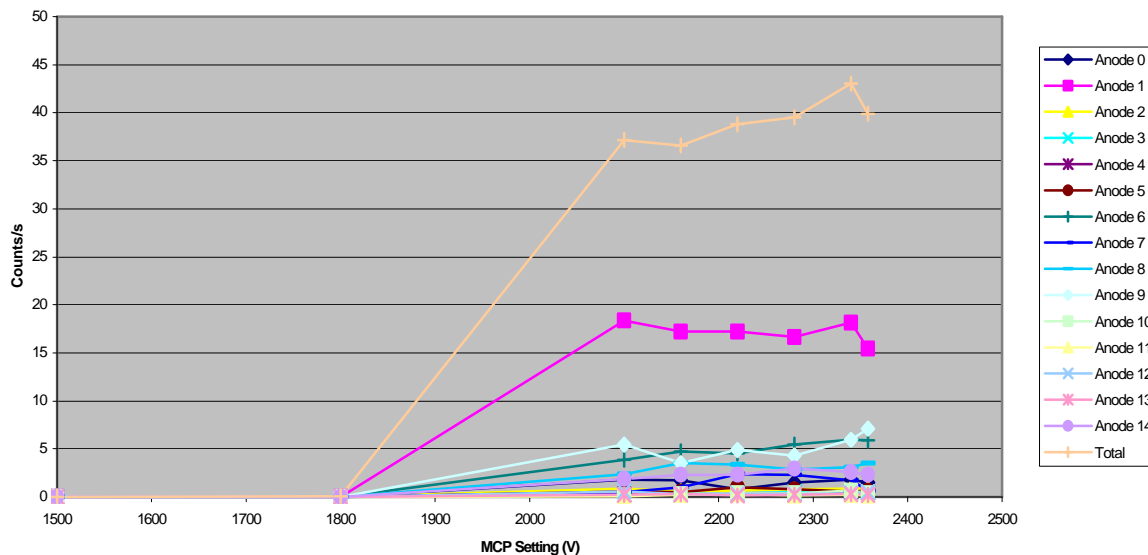


Figure 8.1: ELS background count-rates during power-up on December 17th 2001

9. Deadtime calculation

An experiment to measure the detector deadtime was performed on December 10th 2001. Data was collected for Anode 9 in a 1keV electron beam. A range of electron beam intensities was obtained by stopping down the electron gun UV exciting source by means of neutral density filters (see Table 9.1). Single filters (rather than combinations of filters) were used for each experiment.

The basic equation for deadtime (“Nuclear Electronics”, P.W. Nicholson, pub. Wiley) is:

$$R_{in} - R_{out} = R_{in}R_{out}\tau \tag{1.1}$$

where R_{in} = Input countrate

R_{out} = Counts which the detector actually outputs

τ = Deadtime

Table 9.1: Summary of filters used in deadtime tests

Filename	Filter Nominal OD	OD at $\lambda=253.7\text{nm}^*$	Transmission at $\lambda=253.7\text{nm}$
DED3	2.0	2.13	.00748
DED5	1.0	0.833	0.147
DED6	0.5	0.427	0.374
DED8	0.1	0.162	0.689
DED9	0 (no filter)	0.0	1.00

*According to MSSL report, “Cluster and Cassini Dead Times”, Dave Walton, 1st July 1997

Equation 1.1 can be rearranged to give:

$$R_{in} = R_{out}/(1-R_{out}\tau) \tag{1.2}$$

or:

$$1/R_{out} = (1/R_{in}) + t \quad (1.3)$$

We can replace R_{in} by $R_{in0}t$, where R_{in0} is a reference value of R_{in} (the input count-rate with no filter) and t is the transmission factor of the neutral density filter. Rearranging Equation 1.2 then gives:

$$R_{out}/t = -R_{in0}R_{out}t + R_{in0} \quad (1.4)$$

Equation 1.4 is of the form $y=mx + c$ so plotting R_{out}/t versus R_{out} should give a straight line with gradient $-R_{in0}\tau$ and intercept on the y-axis R_{in0} .

A beam of energy 1keV directly facing Anode 9 was used for this test. Elevation angle and sweep voltage were set at the peak of the distributions for this beam energy (see Calibration Report Volume 2) of 0° and 137.1V respectively. The data is plotted in Figure 9.1.

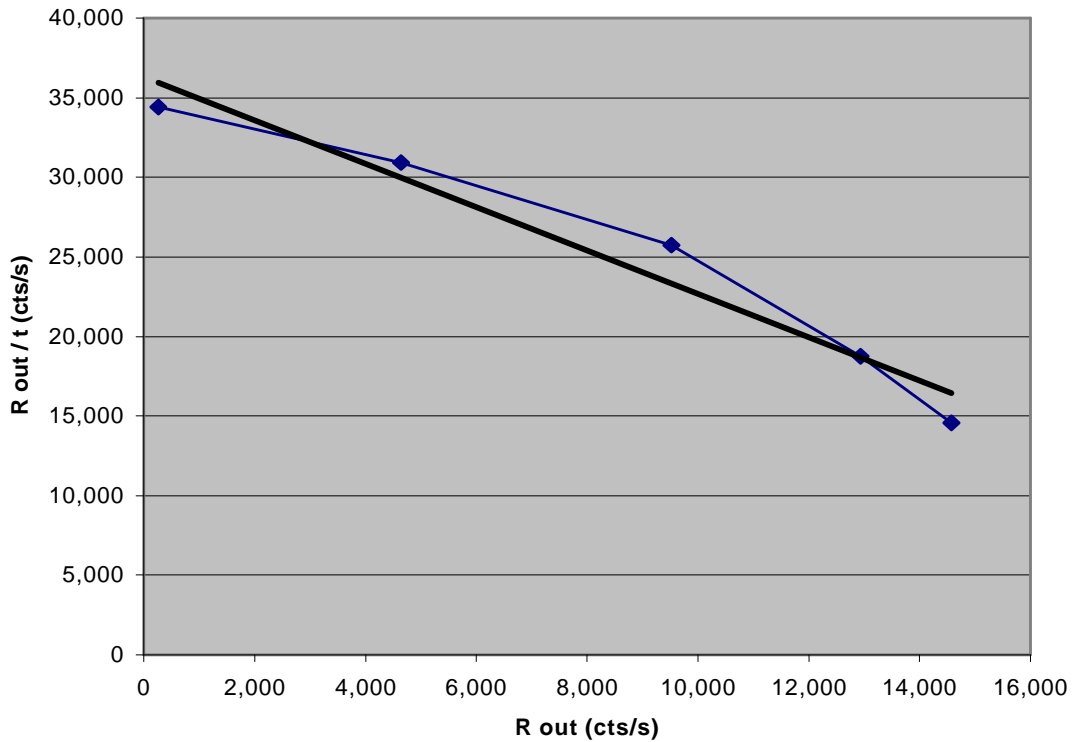


Figure 9.1: ELS deadtime test data December 10th 2001

The data is fitted to a straight line of gradient 1.38 and intercept on the y-axis of 36,207. This gives a value for the instrument deadtime of 38.0 μ s.

If we consider the two possible extremes in possible gradient for the graph represented by (a) the 2 right-most points and (b) the 2 left-most points, we obtain values for the deadtime of 48.5 μ s and 22.6 μ s respectively. The region of the plot with least gradient actually corresponds best to the count-rate regime during ELS calibration (i.e. up to ~5,000 cts/sec per anode) so a value of 22.6 μ s will be used to correct the raw ELS data in all subsequent analysis.

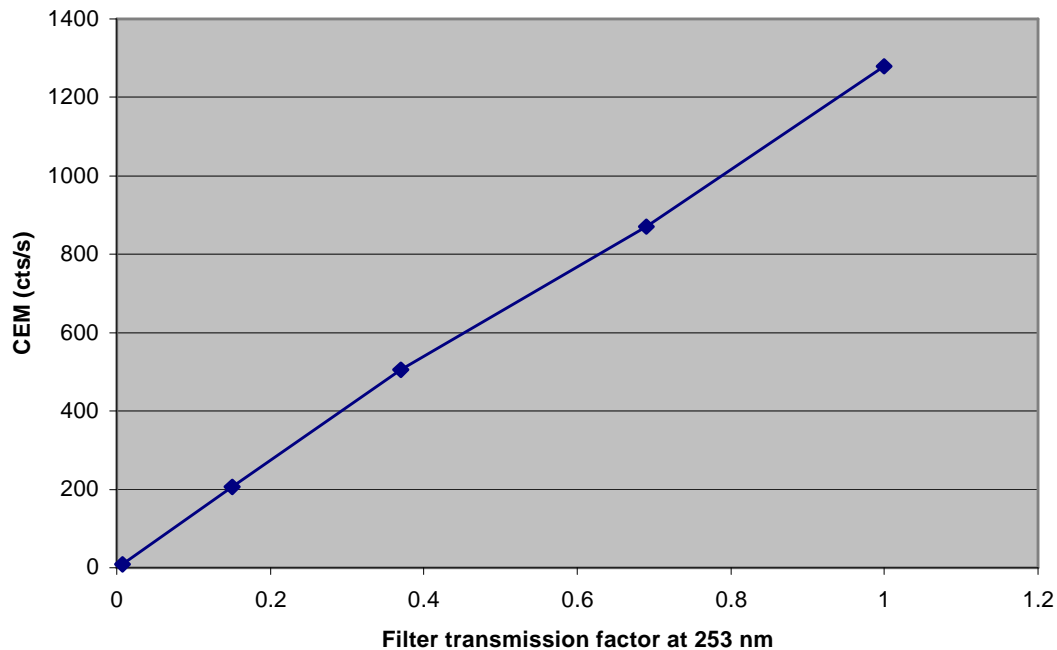


Figure 9.2: CEM counts versus filter transmission

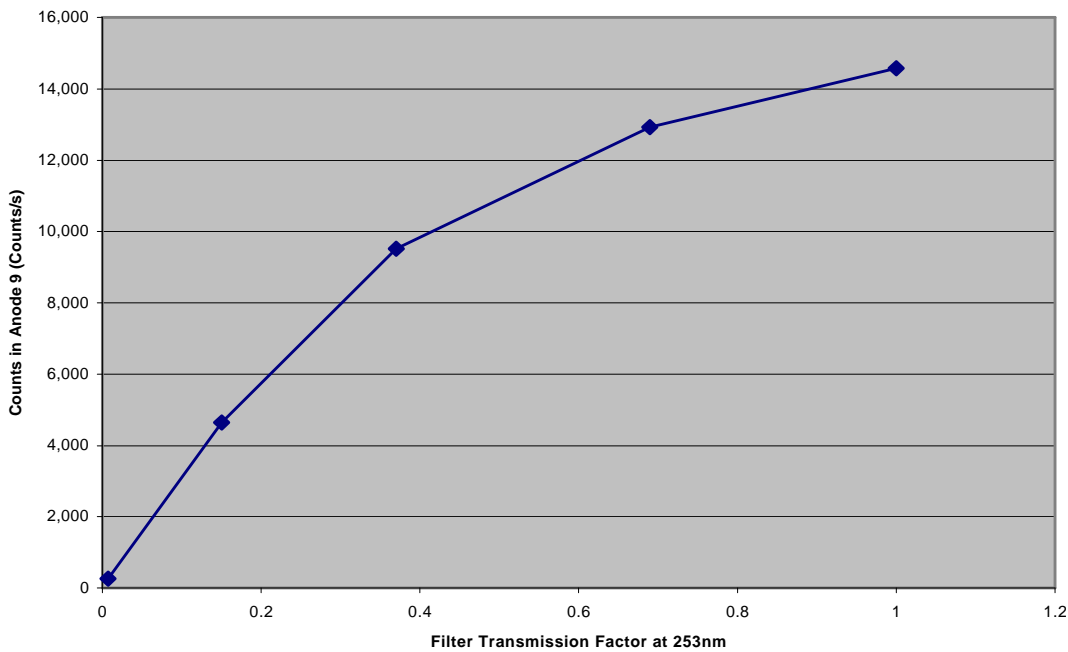


Figure 9.3: ELS counts versus filter transmission

10. Beam characterization

10.1 Beam energy 1.0 keV

Following completion of ELS testing, the beam was characterized using a CEM mounted on an X-Y table. The format of the PACIDERM file used to record the profile of the 1keV beam is given in Table 10.1.1.

Filename	AFBP1K0A.PAC/PDT
Date	Jan 10 th 2002
Beam Energy (eV)	1.0 keV
CEM Level (Volts)	2,400
X dimension (mm)	0 / 140 / step 10
Y dimension (mm)	0 / 140 / step 10
Acquisition Length (seconds)	1
No. of Acquisitions at each point	5

Table 10.1.1: Beam characterization file AFBP1K0A.PAC

The data recorded in AFBP1K0A.PDT is plotted in Figure 10.1.1.

A higher resolution grid of measurements was recorded in the 1.0 keV beam. The file is described in Table 10.1.2. The data is plotted in Figure 10.1.2.

Filename	AFBP1K0B.PAC/PDT
Date	Jan 10 th /11 th 2002
Beam Energy (eV)	1.0 keV
CEM Level (Volts)	2,400
X dimension (mm)	0 / 140 / step 2
Y dimension (mm)	0 / 140 / step 2
Acquisition Length (seconds)	1
No. of Acquisitions at each point	5

Table 10.1.2: Higher resolution beam characterization file AFBP1K0B.PAC

Program dscemprof1.pro

afbp1k0a.pdt, 10/01/02,

DSCEM@2400, 1kV, aperture 0.3mm ?, FILTER = 1.0, 140x140 step 10mm

dummy

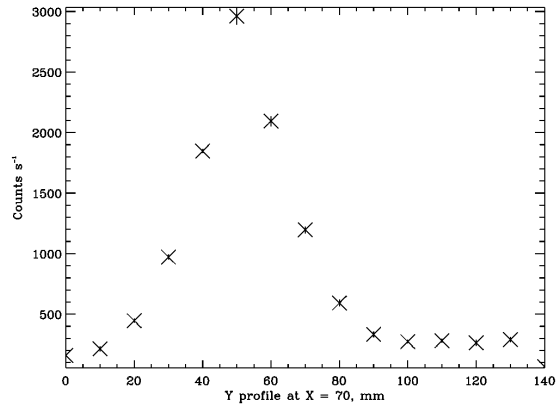
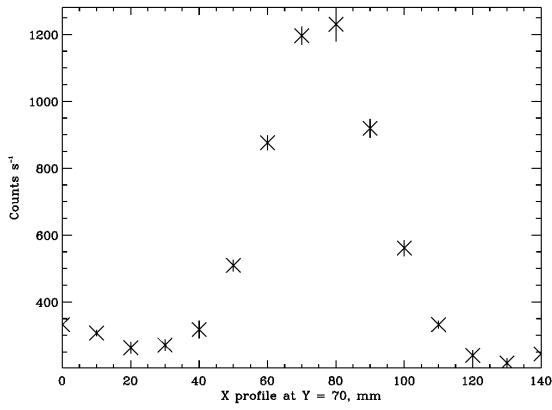
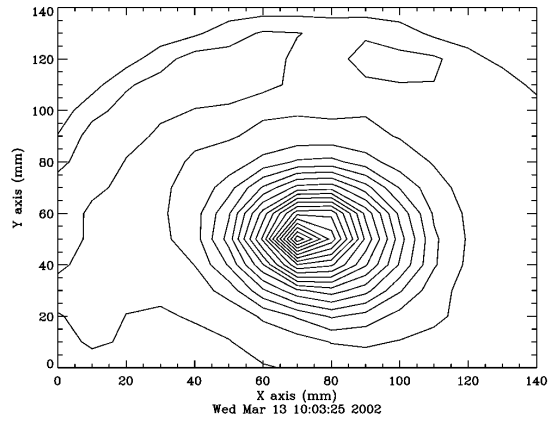
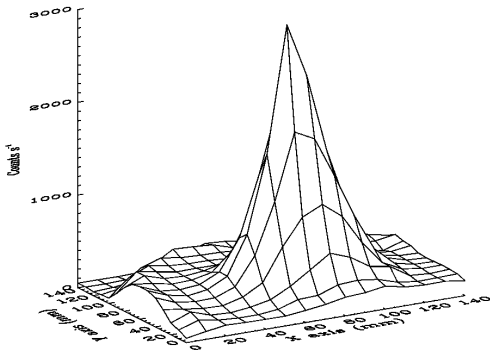
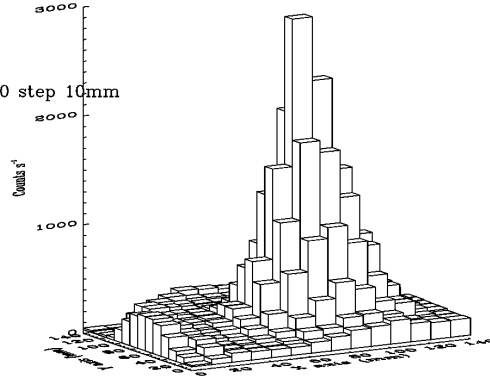


Figure 10.1.1: Beam profile at 1.0 keV beam energy (AFBP1K0A.PDT)

Program dscemprof1.pro

afbp1k0b.pdt, 10/01/02,

DSCEM@2400, 1kV, aperture 0.3mm ?, FILTER = 0.03, 140x140 step 2mm

dummy

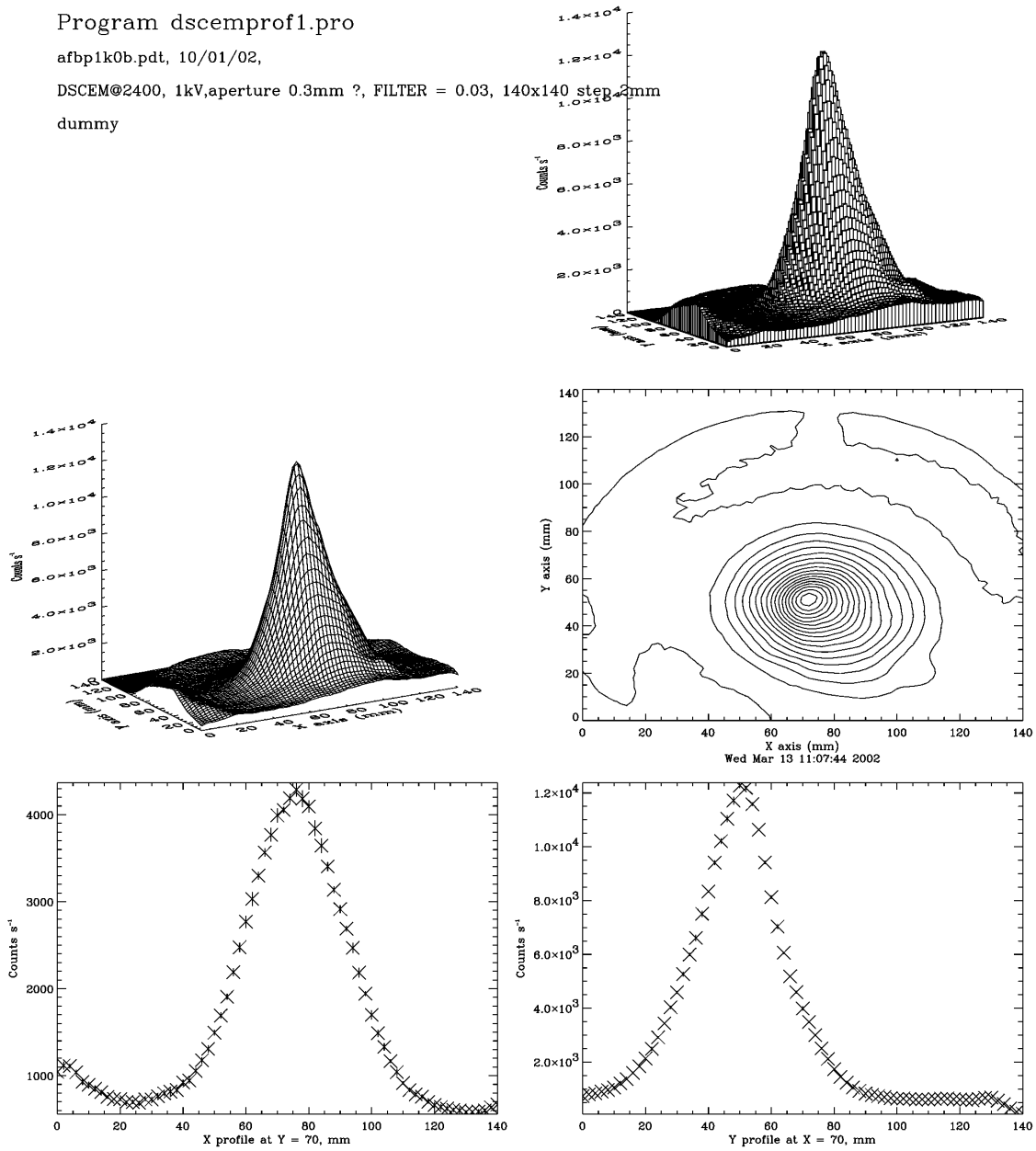


Figure 10.1.2: Higher resolution beam profile at 1.0 keV beam energy (AFBP1K0B.PDT)

10.2 Beam Energy 3.0 keV

Beam characterization was performed at 3.0 keV using a file with the same format as AFBP1K0A.PAC. The data is plotted in Figure 10.2.1.

Program dscemprof1.pro

afbp3k0a.pdt, 10/01/02,

DSCEM@2400, 3kV, aperture 0.3mm ?, FILTER = 1.0, 140x140 step 10mm

dummy

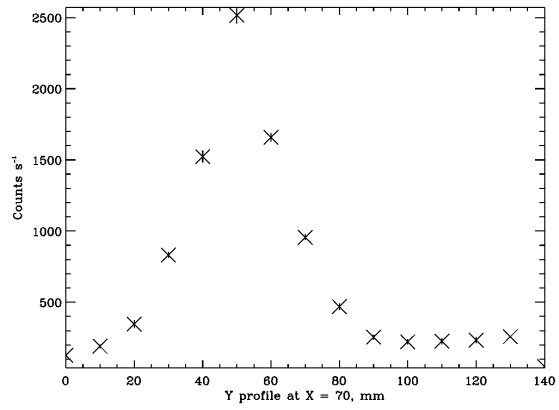
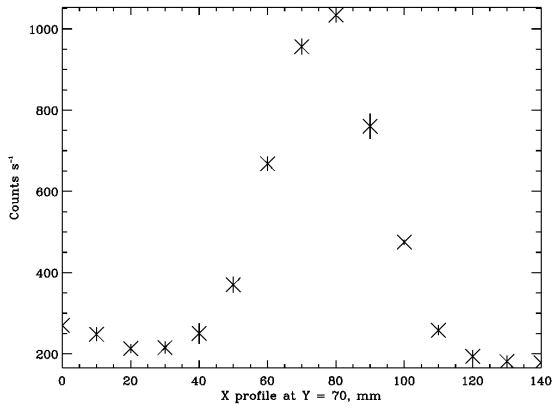
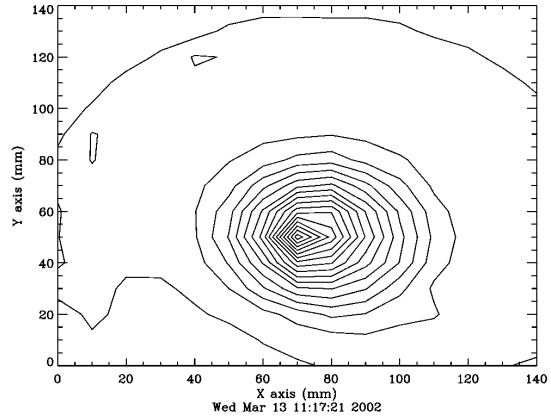
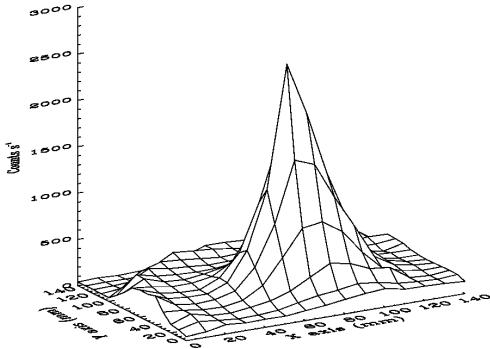
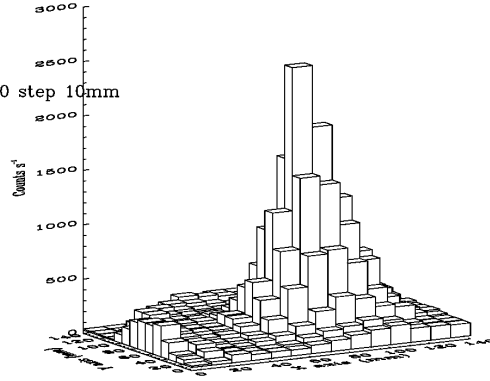


Figure 10.2.1: Beam profile at 3.0 keV beam energy (AFBP3K0A.PDT)

10.3 Beam Energy 10.0 keV

Beam characterization was performed at 10.0 keV using a file with the same format as AFBP1K0A.PAC. The data is plotted in Figure 10.3.1.

```

Program dscemprof1.pro
afbp10ka.pdt, 10/01/02,
DSCEM@2400, 10kV, aperture 0.3mm ?, FILTER = 1.0, 140x140 steps, 10mm
dummy
    
```

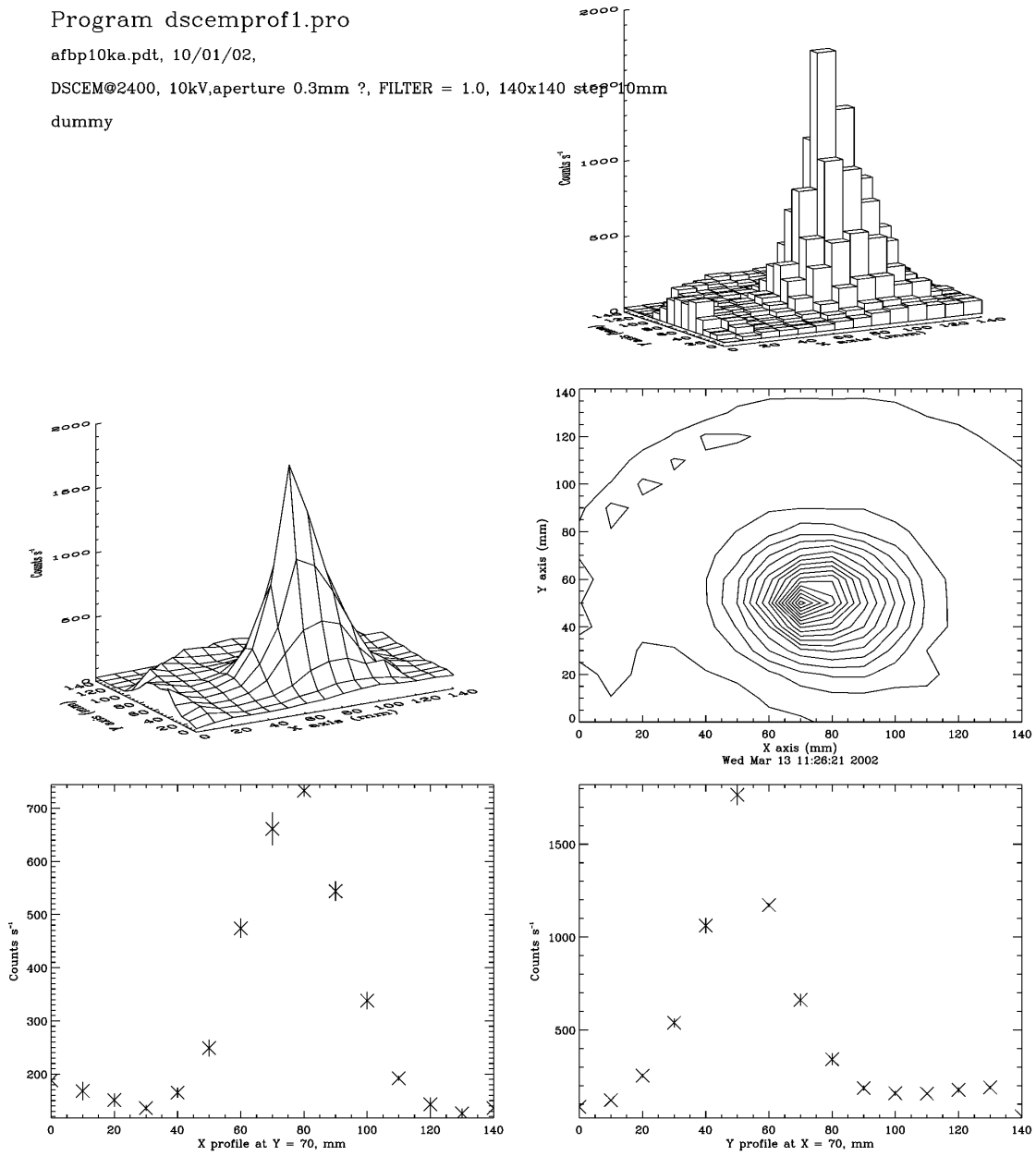


Figure 10.3.1: Beam profile at 10.0 keV beam energy (AFBP10KA.PDT)

The same file was repeated but with Filter = 0.03 (Figure 10.3.2).

Program dscemprof1.pro

afbp10kb.pdt, 11/01/02,

DSCEM@2400, 10kV, aperture 0.3mm ?, FILTER = 0.03, 140x140 step 10mm

dummy

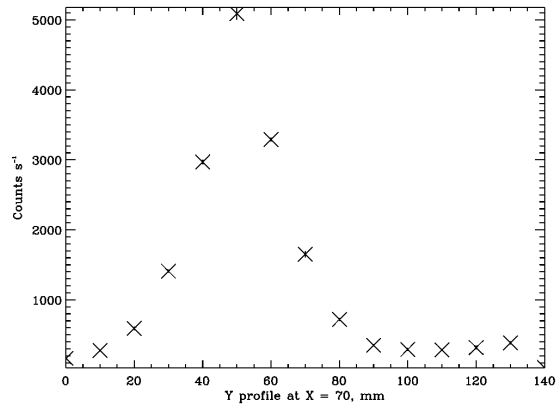
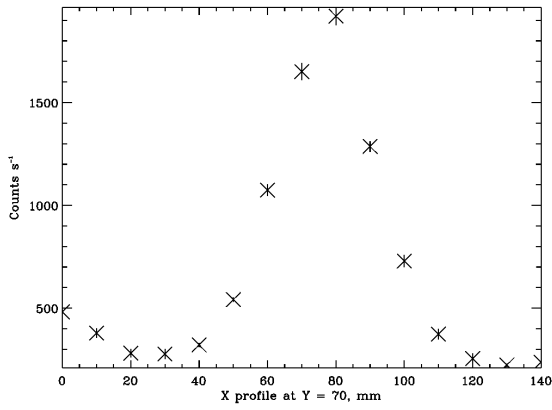
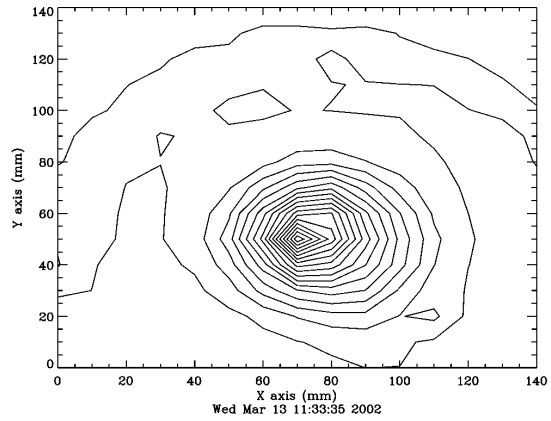
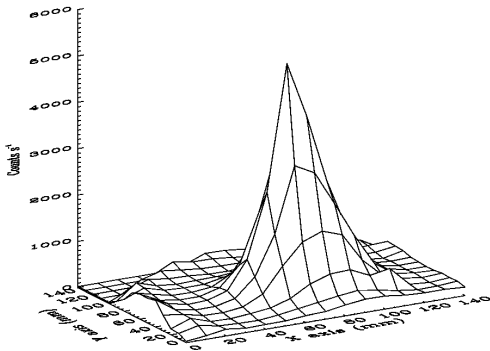
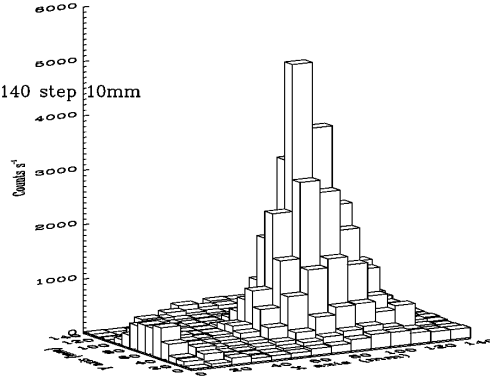


Figure 10.3.2: Beam profile at 10.0 keV beam energy (AFBP10KB.PDT)

10.4 Beam Energy 30 eV

Beam characterization was performed at 30 eV using a file with the same format as AFBP1K0A.PAC. The data is plotted in Figure 10.4.1.

```
Program dscemprof1.pro  
afbp030a.pdt, 10/01/02,  
DSCEM@2400, 30eV, aperture 0.3mm ?, FILTER = 1.0, 140x140 step 10mm  
dummy
```

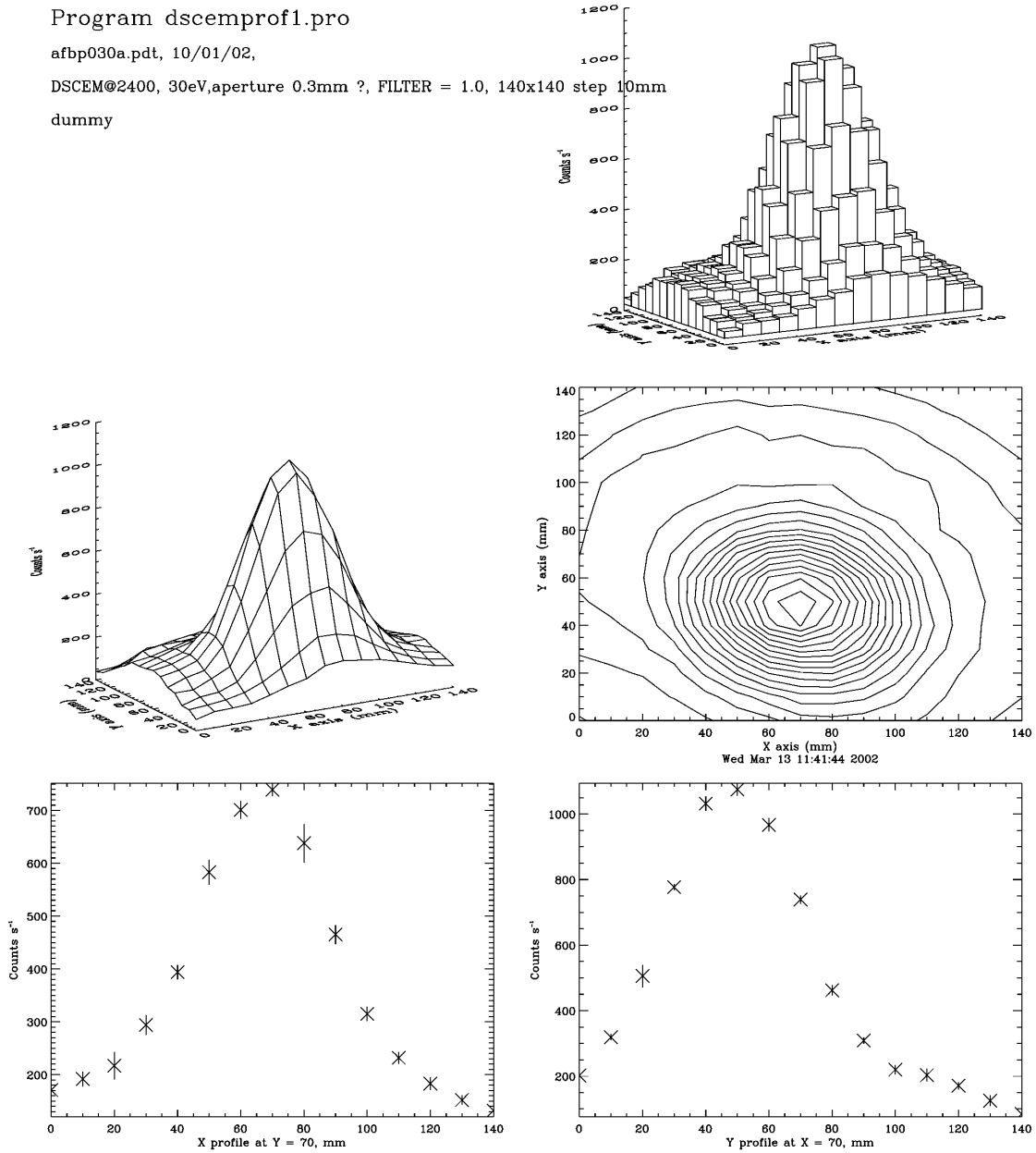


Figure 10.4.1: Beam profile at 30 eV beam energy (AFBP030A.PDT)

The same file was repeated but with Filter = 0.03 (Figure 10.4.2).

Program dscemprof1.pro

afbp030b.pdt, 11/01/02,

DSCEM@2400, 30eV, aperture 0.3mm ?, FILTER = 0.03, 140x140 step

dummy

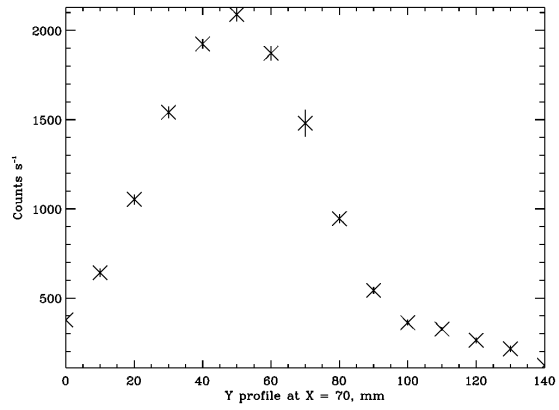
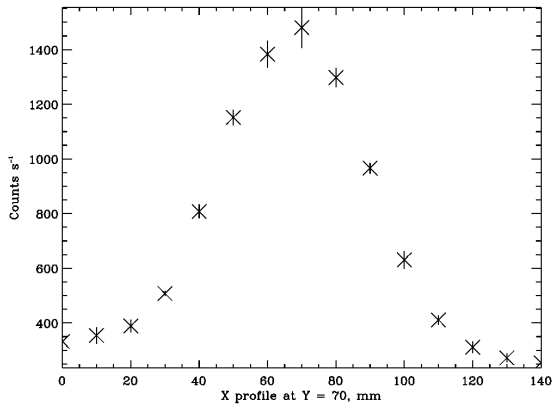
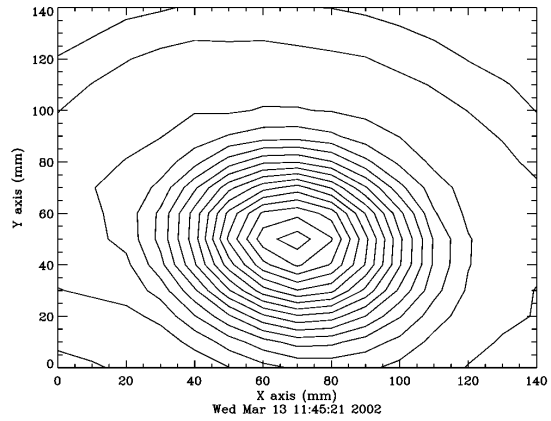
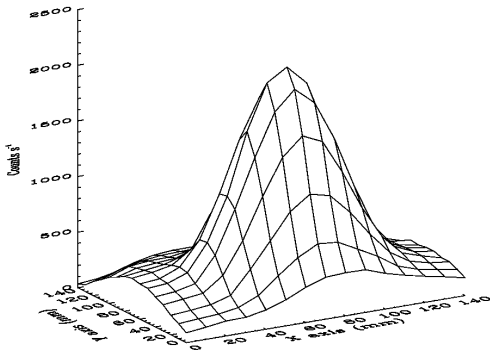
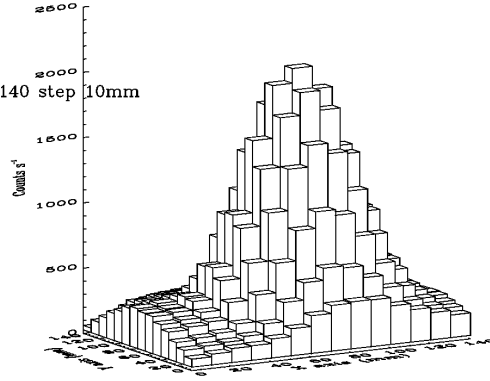


Figure 10.4.2: Beam profile at 30 eV beam energy (AFBP030B.PDT)

10.5 Beam Energy 100 eV

Beam characterization was performed at 100 eV using a file with the same format as AFBP1K0A.PAC. The data is plotted in Figure 10.5.1.

```
Program dscemprof1.pro  
afbp100a.pdt, 10/01/02,  
DSCEM@2400, 100eV, aperture 0.3mm ?, FILTER = 1.0, 140x140 step 10mm  
dummy
```

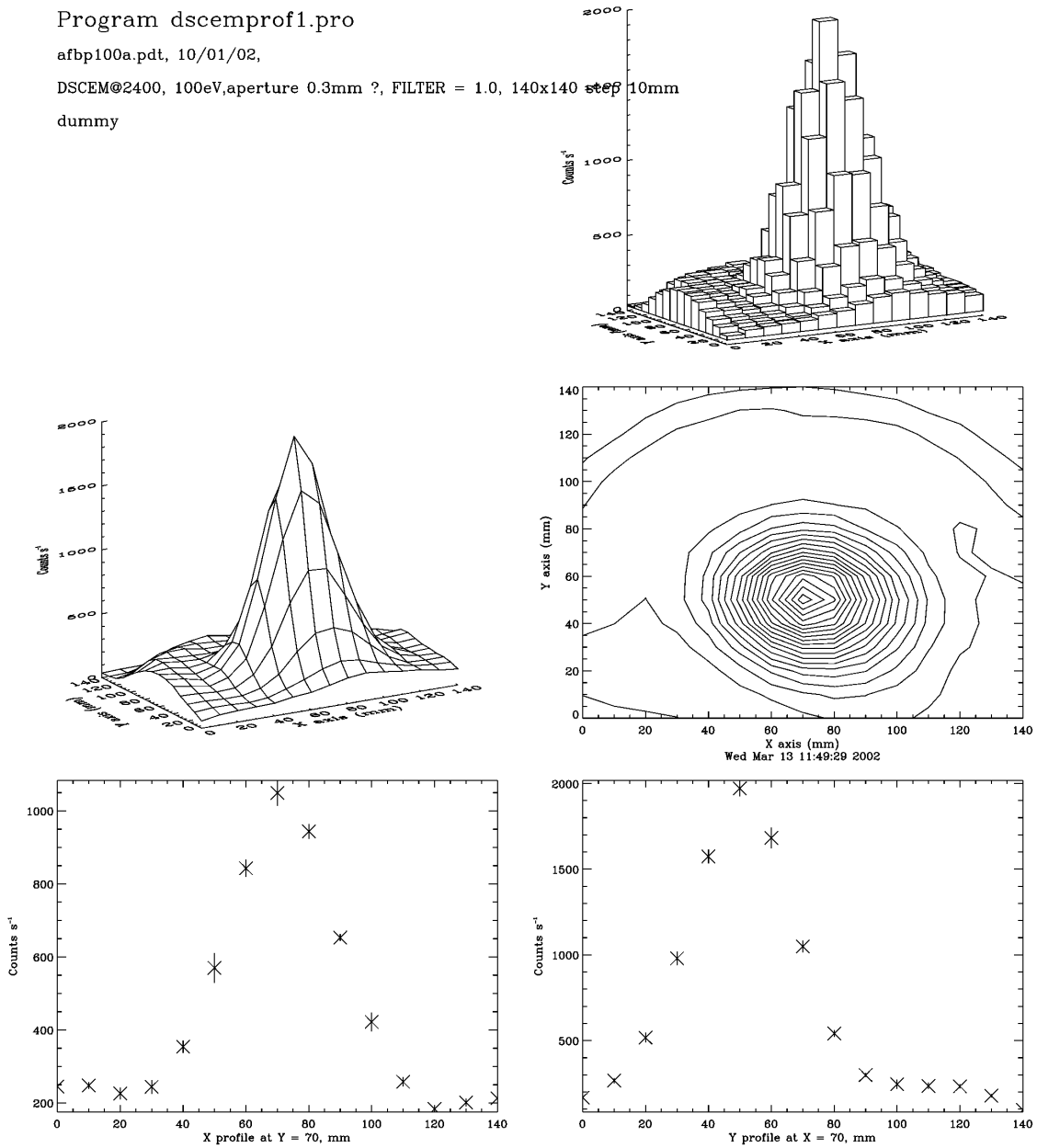


Figure 10.5.1: Beam profile at 100 eV beam energy (AFBP100A.PDT)

Appendix A Power On Procedure

Following is the procedure for power-up of Mars Express ELS during calibration activities at MSSSL.

Date:
Time:
Personnel:

Step No.	Activity	Check
	Turn on UV lamp (ensure shutter is closed) and CEM.	
1	Ensure that chamber pressure interlock is connected.	
2	Check that all cables are connected to the IRF Interface Box etc.	
3	Power on motor driver box, CEM rack, Anode 15 etc.	
4	Power on PC and beam.	
5	Confirm that chamber pressure is less than 2×10^{-6} mbar. Record pressure.	
6	Confirm that all power rails on the IRF Interface Box (IIB) i.e. +5V, -5V, +12V, -12V, +30V, are disabled.	
7	Select desired sweep range on IIB (High/Low).	
8	Confirm that ELS is in safe state (run PACIDERM file FUOFF.PAC)	
9	Power on meters.	
10	Switch on IRF power supply (-5V, +30V, +5V, +12V, -12V, Enable, Range)	
11	Enable +5V, -5V on the IIB.	
12	Enable +12V, -12V on the IIB.	
13	Enable +30V on the IIB.	
14	Confirm the power rail currents are as below:	

Power Rail	Expected Current (mA)	Measured Current (mA)
+5V	10.9 – 12.9	
-5V	14.9 – 17.7	
+12V	20.1 – 58.3	
-12V	1.9 – 2.4	
+30V	0.09 – 0.50	

15	Record CEM counts/second					
----	--------------------------	--	--	--	--	--

16	Confirm that MCP HV monitor = 0.00V.	
17	Confirm that Sweep HV monitor = 0.00V.	
18	Power on line driver power supply (+5V, ~66mA)	
19	Power on MCPs via PACIDERM file AFON235x.PAC. Record filename. Confirm that MCP monitor values are as below:	

DAC Intended Value (V)	Expected MCP HV Monitor Value (V)	Expected actual voltage on MCPs (V)	Measured MCP HV Monitor Value (V)	Measured ELS Counts (per 10 seconds over all anodes)	
0.0	0.00	0			
0.5	0.45	300			
1.0	0.90	600			
1.5	1.35	900			
2.0	1.80	1,200			
2.5	2.25	1,500			
3.0	2.70	1,800			
3.5	3.15	2,100			
3.6	3.24	2,160			
3.7	3.33	2,220			
3.8	3.42	2,280			
3.93	3.54	2,358			

20	Confirm that Sweep monitor value = 0.9 x set DAC level. Note: For high range, actual Sweep Voltage = 560 x set DAC level. For low range, actual Sweep Voltage = 4.198 x set DAC level.	
----	--	--

Power Off Procedure

Following is the procedure for power-off of Mars Express ELS during calibration activities at MSSSL.

Date:
Time:
Personnel:

Step No.	Activity	Check
1	Replace the UV shutter.	<input type="checkbox"/>
2	Turn off the beam HV supply.	<input type="checkbox"/>
3	Turn off the UV.	<input type="checkbox"/>
4	Power off MCPs via PACIDERM file AFMCPOFA .PAC.	<input type="checkbox"/>
5	Confirm that MCP HV monitor = 0.00V.	<input type="checkbox"/>
6	Confirm that Sweep HV monitor = 0.00V.	<input type="checkbox"/>
7	Power off line driver power supply.	<input type="checkbox"/>
8	Disable +30V on the IIB.	<input type="checkbox"/>
9	Disable +12V, -12V on the IIB.	<input type="checkbox"/>
10	Disable +5V, -5V on the IIB.	<input type="checkbox"/>
11	Switch off IRF power supply.	<input type="checkbox"/>
12	Switch off multimeters.	<input type="checkbox"/>
13	Record the setting for the CEM.	<input type="checkbox"/>
14	Power off motor driver and CEM.	<input type="checkbox"/>
15	Record chamber pressure.	<input type="checkbox"/>